CONFORMAL MAPPING OF A CLASS OF DOUBLY CONNECTED REGIONS

by

Patricio A. Laura

Technical Report No. 8

National Aeronautics and Space Administration

Research Grant No. NsG-125-61 (Suppl. 3)

JANUARY 1965

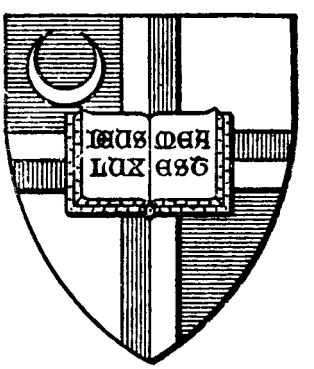

THE CATHOLIC UNIVERSITY OF AMERICA
WASHINGTON, D.C. 20017

CONFORMAL MAPPING OF A CLASS OF DOUBLY CONNECTED REGIONS

By

Patricio A. Laura

Technical Report No. 8

to the

NATIONAL AERONAUTICS AND SPACE ADMINISTRATION
Washington 25, D. C.

Under Research Grant No. NsG-125-61 (Suppl. 3)

January 1965

THE CATHOLIC UNIVERSITY OF AMERICA
Washington, D. C. 20017

CONFORMAL MAPPING OF A CLASS OF DOUBLY CONNECTED REGIONS*

Abstract

It is shown in the present investigation that the system of two integral equations obtained by Kantorovitch and Muratov for the conformal mapping of an arbitrary, finite, doubly connected region onto a circular annulus simplifies considerably when the configuration has one or more axes of symmetry and one of the boundaries is a circle. Once the correspondence between boundary points is established the function which maps the annulus B_ξ in the ξ-plane onto the given domain B_z in the z-plane is obtained by a procedure of successive approximations. The method is illustrated in several cases where the web fraction is close to one.

Table of Contents

---

*Based on a dissertation submitted to the Faculty of the Graduate School of Arts and Sciences of the Catholic University of America in Partial Fulfillment of the Requirements for the Degree of Doctor of Philosophy

INTRODUCTION

Solution of a large number of problems of importance in modern technology hinges critically on the possibility of conformal transformation of a doubly connected region onto a circular annulus. For example, the analysis of stresses in a solid propellant rocket grain by means of complex variable techniques requires the conformal transformation of an annulus onto a region with a circular external boundary and an internal boundary which generally consists of several identical and symmetrical parts which form a star shaped configuration. Wilson [1][1] has solved this problem in the case that the web fraction[2] is relatively small. It can be shown that Wilson's approach leads to large error in mapping the external circle when the web fraction exceeds certain values which depend upon the number of axes of symmetry.

For example, Arango [2] has shown that for four axes of symmetry the error increases rapidly when the web fraction increases beyond 0.5. When the web fraction reaches the value 0.90, the outer boundary has lost all semblance of a circle. This error arises due to the fact that Wilson and Arango treated the conformal transformation of an infinite domain

---

[1]Numbers in brackets designate References at the end of the paper.

[2]Web fraction w in defined as the ratio of the diameter of the circle circumscribing the inner boundary of a doubly connected region to the diameter of the circle circumscribing the outer boundary.

with a hole onto another such region. Consequently, while the mapping function accurately transforms the unit circle in the ξ-plane into the internal boundary in the z-plane, the external boundary transforms only approximately into a circle.

However the approximation can be very accurate provided the web fraction is sufficiently small. This concern with the accuracy of the transformation of the external boundary is of substantial importance since, while the web fraction may be sufficiently small in the unburned solid propellant grain, it will increase toward unity as a consequence of the burning process. It should be clear, therefore, that it is essential to develop techniques for the conformal transformation of finite, doubly connected domains.

Kantorovitch and Muratov [3] have shown that the problem of conformal transformation of an arbitrary, finite, doubly connected region onto a circular annulus can be reduced to the solution of two coupled integral equations for the unknown functional dependence

$$\theta_i = \theta_i(\emptyset_i) \qquad (i = 1,2)$$

where the subscripts 1 and 2 designate the inner and outer contour, respectively; and $\emptyset$ and θ are the arguments in the z and ξ planes, respectively. (See Fig. 1). If the configuration has one or more axes of symmetry and one of the boundaries is a circle, it is shown in this investigation that the system of two integral equations simplifies considerably.

Once $\theta_i = \theta_i(\emptyset_i)$ is obtained Kantorovitch and Muratov [3] derived a straight forward technique for determining the conformal transformation

$$\xi = \xi(z)$$

However for convenience in applications (mathematical theory of elasticity, vibrations, etc.), it is important to know the function which maps an annulus onto the given shape; i.e.,

$$z = z(\xi)$$

Clearly, if $\xi = \xi(z)$ is known, in principle, one could determine $z = z(\xi)$. However, it is more convenient to determine $z = z(\xi)$ directly once both integral equations are solved.

DERIVATION OF THE INTEGRAL EQUATIONS

Let us consider an arbitrary, finite, doubly connected domain B_z in the z-plane. (See Fig. 1). We denote by $\xi = f(z)$ the function which maps B_z into the circular annulus B_ξ in the ξ-plane; the curve C_2 transforms into the unit circle and C_1 into the circle $|\xi| = \rho_1 < 1$. We define

$$F(z) = \ln f(z) = \ln\xi = \ln\rho + i\theta \tag{1}$$

wherein, for emphasis, we point out that z represents a generic point in B_z.

Introducing a cut L in the domain B_z (see Fig. 2) and applying the Cauchy integral formula results in

$$F(z) = \frac{1}{2\pi i}\left\{\oint_{C_2}\frac{F(t)}{t-z}\,dt - \oint_{C_1}\frac{F(t)}{t-z}\,dt + \underset{(L^+)}{\int_{z_2}^{z_1}}\frac{F(t)}{t-z}\,dt + \underset{(L^-)}{\int_{z_1}^{z_2}}\frac{F(t)}{t-z}\,dt\right\} \tag{2}$$

$F(z)$ is not single valued in B_z; with every cycle around C_1 the imaginary part increases by $2\pi i$. Consequently,

$$\Sigma = \frac{1}{2\pi i}\left\{\underset{(L^+)}{\int_{z_2}^{z_1}}\frac{F(t)}{t-z}\,dt + \underset{(L^-)}{\int_{z_2}^{z_1}}\frac{F(t)}{t-z}\,dt\right\} \neq 0 \tag{3a}$$

In order to calculate its value we can express $\sum$ in the following form:

$$\sum = \frac{1}{2\pi i}\int_{z_1}^{z_2} \frac{(F(t)|_{L^-} - F(t)|_{L^+})\, dt}{t-z} \tag{3b}$$

But

$$F(t)\Big|_{L^-} = \ln\rho + i\theta \tag{3c}$$

and

$$F(t)\Big|_{L^+} = \ln\rho + i(\theta + 2\pi) \tag{3d}$$

Thus

$$F(t)\Big|_{L^-} - F(t)\Big|_{L^+} = -2\pi i$$

and Eq. (3b) becomes

$$\sum = -\int_{z_1}^{z_2} \frac{dt}{t-z} = -\ln\frac{z_2 - z}{z_1 - z} \tag{3e}$$

Substituting Eq. (3e) in Eq. (2) we obtain

$$F(z) = \frac{1}{2\pi i}\oint_{C_2}\frac{F(t)}{t-z}\,dt - \frac{1}{2\pi i}\oint_{C_1}\frac{F(t)}{t-z}\,dt - \ln\frac{z_2 - z}{z_1 - z} \qquad (4a)$$

For points on C_2 we define

$$F(z) = \ln\rho_2 + i\theta_2(\sigma_2) = i\theta_2(\sigma_2)$$

since $\rho_2 = 1$; and for points on C_1 we define

$$F(z) = \ln\rho_1 + i\theta_1(\sigma_1)$$

wherein σ_1 and σ_2 denote the arc lengths on the boundaries C_1 and C_2 respectively, from arbitrary fixed points on the respective boundaries to the points under consideration. Thus the first term on the right hand side of (4a) becomes:

$$\frac{1}{2\pi i}\oint_{C_2}\frac{F(t)}{t-z}\,dt = \frac{1}{2\pi}\oint_{C_2}\frac{\theta_2(\sigma_2)}{t-z}\,dt$$

Similarly the second term results in:

$$-\frac{1}{2\pi i}\oint\frac{F(t)}{t-z}\,dt = -\frac{1}{2\pi i}\oint\frac{\ln\rho_1}{t-z}\,dt - \frac{1}{2\pi}\oint_{C_1}\frac{\theta_1(\sigma_1)}{t-z}$$

The expression $\oint_{C_1}\frac{\ln\rho_1}{t-z}\,dt$ vanishes identically since

ρ_1 is a constant and the integrand is analytic within and on the boundary of C_1 (Cauchy-Goursat Theorem). Thus Eq. (4a) can be written:

$$F(z) = \frac{1}{2\pi}\oint_{C_2} \frac{\theta_2(\sigma_2)}{t-z}\,dt - \frac{1}{2\pi}\oint_{C_1} \frac{\theta_1(\sigma_1)}{t-z}\,dt - \ln\frac{z_2-z}{z_1-z} \quad (4b)$$

This equation can be more conveniently written if we use the following relations (see Figure 2).

$$t-z = \left|t-z\right| e^{i\omega} = re^{i\omega}$$
$$z_1-z = r_1e^{i\omega_1}$$
$$z_2-z = r_2e^{i\omega_2}$$
$$\omega_2-\omega_1 = \beta$$
$$\alpha-\omega = \pi/2-(n_t,r)$$

where α is the angle between the positive counterclockwise direction of the tangent to the boundary C_i and the positive direction of the real axes, ω is the angle between r and the positive direction of the real axes and n_t is the inwardly directed normal to the boundary C_i. Additionally we define:

$$dt = \left|dt\right| e^{i\alpha}$$

or $dt = d\sigma \cdot e^{i\alpha}$ wherein $dt = \left|d\sigma\right|$ is the magnitude of a differential element of the boundary C_i. Making use of these definitions we can express dt/t-z as follows:

$$\frac{dt}{t-z} = \frac{e^{i\alpha}}{re^{i\omega}} d\sigma = \frac{d\sigma}{r} e^{i[\pi/2 - (n_t, r)]} = i \frac{d\sigma}{r} e^{-i(n_t, r)}$$

Similarly:

$$\ln \frac{z_2 - z}{z_1 - z} = \ln \frac{r_2}{r_1} e^{i(\omega_2 - \omega_1)} = \ln \frac{r_2}{r_1} e^{i\beta} = \ln \frac{r_2}{r_1} + i\beta$$

Now, Eq. (4b) becomes:

$$F(z) = i \frac{1}{2\pi} \oint_{C_2} \frac{\theta_2(\sigma_2) e^{-i(n_t, r)}}{r} d\sigma_2 - i \frac{1}{2\pi} \oint_{C_1} \frac{\theta_1(\sigma_1) e^{-i(n_t, r)}}{r} d\sigma_1 -$$

$$- \ln \frac{r_2}{r_1} - i\beta \qquad (4c)$$

Equating the imaginary parts of (4c) we obtain:

$$\theta = \frac{1}{2\pi} \oint_{C_2} \frac{\theta_2(\sigma_2) \cos(n_t, r) d\sigma_2}{r} - \frac{1}{2\pi} \oint_{C_1} \frac{\theta_1(\sigma_1) \cos(n_t, r) d\sigma_1}{r} - \beta$$

(5a)

wherein Eq. (1) has been used. If the point z is located on C_2 the first term of Eq. (5a) becomes:

$$\frac{1}{2\pi}\left[\oint_{C_2} \frac{\theta_2(\sigma_2)\cos(n_t, r)}{r} d\sigma_2 + \pi\theta_2(\sigma_2)\right] \tag{5b}$$

This is a well known result in the theory of the potential. *Thus, Eq. (5a) becomes

$$\theta_2(\sigma_2) = -2\beta(\sigma_2) + \frac{1}{\pi}\oint_{C_2} \frac{\theta_2(\sigma_2)\cos(n_t, r)}{r} d\sigma_2$$

$$-\frac{1}{\pi}\oint_{C_1} \frac{\theta_1(\sigma_1)\cos(n_t, r)}{r} d\sigma_1 \tag{6a}$$

If now the point z moves to C_1 the integral

$$\frac{1}{2\pi}\oint_{C_1} \frac{\theta_1(\sigma_1)\cos(n_t, r)}{r} d\sigma_1$$

*See Appendix.

becomes

$$\frac{1}{2\pi}\left[\oint_{C_1} \frac{\theta_1(\sigma_1)\cos(n_t, r)\,d\sigma_1}{r} - \pi\theta_1\right]$$

and we obtain the second integral equation.

$$\theta_1(\sigma_1) = \frac{1}{\pi}\oint_{C_2} \frac{\theta_2(\sigma_2)\cos(n_t, r)\,d\sigma_2}{r} - \frac{1}{\pi}\oint_{C_1} \frac{\theta_1(\sigma_1)\cos(n_t, r)\,d\sigma_1}{r} - 2\beta(\sigma_1) \,. \tag{6b}$$

Equations (6) constitute the system of coupled integral equations which we have been seeking. Their solution will yield the functional form of the relations

$$\theta_i = \theta_i(\sigma i) \qquad (i = 1,2)$$

or what is equivalent

$$\theta_i = \theta_i(\phi_i) \qquad (i = 1,2)$$

Let us now simplify Eqs. (6) when C_2 is a circle and the domain B_z has p axes of symmetry. Consider the expression $\frac{\cos(n_t, r)}{r}$ as it appears in the first integral of Eq. (6a). From Fig. 5, since $z \in C_2$

$$r^2 = (x - x_c)^2 + (y - y_c)^2 =$$

$$= R^2\left[(\cos\phi - \cos\phi_c)^2 + (\sin\phi - \sin\phi_c)^2\right] \tag{7}$$

$$r^2 = 2R^2\left[1 - \cos(\phi - \phi_c)\right] \tag{8}$$

where x_c, y_c and ϕ_c are the values of x, y and ϕ at the point z on C_2.

Additionally,

$$\cos(n_t, r) = \cos\phi\cos\omega + \sin\phi\sin\omega \tag{9a}$$

and

$$\cos\omega = \frac{x - x_c}{r} = \frac{R(\cos\phi - \cos\phi_c)}{r} \tag{9b}$$

$$\sin\omega = \frac{y - y_c}{r} = \frac{R(\sin\phi - \sin\phi_c)}{r} \tag{9c}$$

Substituting (9b) and (9c) into (9a) we obtain:

$$\cos(n_t, r) = \frac{R}{r}\left[\cos\phi(\cos\phi - \cos\phi_c) + \sin\phi(\sin\phi - \sin\phi_c)\right]$$

Rearrangement leads to

$$\frac{\cos(n_t, r)}{r} = \frac{R}{r^2}\left[1 - \cos(\phi - \phi_c)\right] \tag{9d}$$

Substituting (8) in (9d) we finally obtain:

$$\frac{\cos(n_t, r)}{r} = \frac{1}{2R} \tag{10}$$

Then, the line integral under consideration becomes:

$$\oint \frac{\theta_2(\sigma_2)\cos(n_t, r)}{r}\, d\sigma_2 = \frac{1}{2R}\oint_{C_2} \theta_2(\sigma_2)\, d\sigma_2$$

so that substitution into Eq. (6a) yields

$$\theta_2(\sigma_2) = -2\beta(\sigma_2) + \frac{1}{2\pi R}\oint_{C_2} \theta_2(\sigma_2)\, d\sigma_2 -$$

$$-\frac{1}{\pi}\oint_{C_1} \frac{\theta_1(\sigma_1)\cos(n_t, r)}{r}\, d\sigma_1 \qquad (11)$$

It should be reemphasized that Eq. (11) is to be used rather than Eq. (6a) when C_2 is a circle. Note that no assumptions of symmetry of the given doubly connected domain have been introduced up to this point.

Further important simplifications can be made in Eq. (11) when symmetry conditions are introduced. For the purpose of making these simplifications it is necessary to study the behaviour of the functional relation

$$\theta_2 = \theta_2(\sigma_2) = \theta_2\ (\phi_2)$$

We now introduce the condition that the domain B_z has p-axes of symmetry. For example, the illustrative domain of Fig. 5 has four axes of symmetry so the p = 4.

We define now:

$$\theta_2\ (\phi_2) = \phi_2 + \chi\ (\phi_2) \qquad (12)$$

Since the configuration has p-axes of symmetry, it is reasonable to expect that $\chi(\phi_2)$ will be a periodic function of period $2\pi/p$.

Furthermore it will be shown that $\chi(\phi_2)$ is an odd function of ϕ_2. Consider a point P (on the outer boundary) with argument ϕ_2. Its image point in the ξ-plane will have an argument θ_2. Because of symmetry, if we take a point $P^{(1)}$ on the outer boundary C_2 with argument $(2\pi/p - \phi_2)$ (See Figure 6), its image point in the ξ -plane will have an argument

$$\left(\frac{2\pi}{p} - \theta_2\right) = \frac{2\pi}{p} - [\phi_2 + \chi(\phi_2)]$$

wherein we have used Eq. (12).

Similarly points $P^{(k)}$ on C_2 with arguments

$$\frac{2k\pi}{p} - \phi_2 \qquad (k = 1,2,\ldots p)$$

will have image points in the ξ -plane with arguments given by

$$\frac{2k\pi}{p} - \theta_2 \qquad (k = 1,2,\ldots p)$$

The point $P^{(p)}$ on C_2 with argument

$$2\pi - \phi_2$$

has an image point in the ξ-plane with argument

$$2\pi - \theta_2 = 2\pi - \phi_2 - \chi(\phi_2)$$

wherein we have used Eq. (12) once again. On the other hand $P^{(p)}$

has an alternative argument $(-\phi_2)$ in the z-plane and its image point in the ξ-plane has the alternative argument

$$-\phi_2 + \chi(-\phi_2)$$

From these alternative expressions for the argument of the image point of $P^{(p)}$ in the ξ-plane we obtain

$$-\phi_2 - \chi(\phi_2) = -\phi_2 + \chi(-\phi_2)$$

or

$$\chi(-\phi_2) = -\chi(\phi_2)$$

Thus $\chi(\phi_2)$ is an odd function of ϕ_2. It can be shown that $\chi(\phi_2)$ complies with the well known Dirichlet conditions; and, therefore can be expanded in a Fourier sine series, i.e.:

$$\chi(\phi_2) = \sum_{n=1}^{\infty} b_n \sin(p n \phi_2) \tag{13}$$

We return once again to the problem of simplifying Eq. (11). In view of Eq. (12) we can write

$$\frac{1}{2\pi R}\oint_{C_2} \theta_2(\sigma_2)\, d\sigma_2 = \frac{1}{2\pi R}\oint_{C_2} \phi_2\, d\sigma_2 + \frac{1}{2\pi R}\oint_{C_2} \chi(\phi_2)\, d\sigma_2$$

Since $d\sigma_2 = R\,d\phi_2$, it follows that

$$\frac{1}{2\pi R}\oint_{C_2} \theta_2(\sigma_2)\,d\sigma_2 = \frac{1}{2\pi}\int_0^{2\pi} \phi_2\,d\phi_2 + \frac{1}{2\pi}\sum_{n=1}^{\infty} b_n \int_0^{2\pi} \sin(p n \phi_2)\,d\phi_2$$

so that

$$\frac{1}{2\pi R}\oint_{C_2} \theta_2(\sigma_2)\,d\sigma_2 = \pi$$

In view of this result, Eq. (11) becomes

$$\theta_2(\sigma_2) = -2\beta(\sigma_2) + \pi - \frac{1}{\pi}\oint_{C_1} \frac{\theta_1(\sigma_1)\cos(n_t, r)}{r}\,d\sigma_1$$

$$z \in C_2 \quad \ldots\ldots (14)$$

In summary, it has been shown that when C_2 is a circle and the domain B_z has p-axes of symmetry, the applicable integral equations are Eqs. (6b) and (14).

By an analogous argument it can be shown that when C_1 is a circle and the domain B_z has p-axes of symmetry, the applicable integral equations are Eq. (6a) and the following

$$\theta_1(\sigma_1) = -2\beta(\sigma_1) + \frac{1}{\pi}\oint_{C_2} \frac{\theta_2(\sigma_2)\cos(n_t, r)}{r}\,d\sigma_2 - \pi$$

$$z \in C_1 \quad \ldots\ldots (15)$$

NUMERICAL SOULUTION OF THE INTEGRAL EQUATIONS

We shall limit all further discussions to cases wherein the outer boundary C_2 of the domain B_z is circular and B_z has p-axes of symmetry. Thus in order to relate ϕ_i, the argument of a point on the boundary C_i of the domain B_z in the z-plane, and θ_i, the argument of the image point on the boundary γ_i of the domain B_ξ in the ξ-plane, we must integrate Eqs. (6b) and (14). Closed form solution of these integral equations seems extremely difficult so we must be satisfied with numerical solution thereof.

The explanation of the numerical procedure is readily presented in terms of a specific example. Therefore we consider the domain B_z of Fig. 7 wherein the inner boundary is square with sides parallel to the coordinate axes. Clearly, B_z has four axes of symmetry so that $p = 4$ in this case. We begin the numerical procedure by subdividing the boundaries C_1 and C_2 into any arbitrary number of small segments which, in general, need not be equal in length. In the specific example we take 40 equally-spaced points on each boundary numbered as shown in Fig. 7. The arc-length between points on C_1 is denoted by $\Delta\sigma_1$ and on C_2 by $\Delta\sigma_2$.

The theoretical development required the introduction of a cut between C_1 and C_2 as shown in Fig. 2. Thus, the next step is to introduce such a cut in B_z of Fig. 7. It will be convenient to take this cut along the positive half of the x-axis. Thus, the cut runs from point 1 on C_1 to point 1 on C_2.

We consider first the integration of Eq. (14). We select a typical point on C_2; for example, the point 2. Associated with this point is its image point, (2) on γ_2. We denote the argument associated with the image point by $\theta_{2,2}$ wherein the first subscript indicates the fact that the point under consideration lies on γ_2 while the second subscript indicates the point itself. Thus, $\theta_{2,6}$ denotes the argument of point 6 on γ_2 and $\theta_{1,11}$ denotes the argument of point 11 on γ_1. We must now construct lines from the ends of the cut through the point under consideration; i.e. lines from point 1 on C_1 and point 1 on C_2 through the point 2 on C_2. The angle enclosed between these lines is the angle $\beta(\sigma_2)$ of Eq. (14) and for numerical purposes it is denoted by $\beta_{2,2}$, see Fig. 7. Now Eq. (14) can be rewritten as follows:

$$\theta_{2,2} = -2\beta_{2,2} + \pi - \frac{1}{\pi}\oint_{C_1} \theta_1(\sigma_1)\,\frac{\cos(n_t, r)}{r}\,d\sigma_1 \tag{16}$$

The angle $\beta_{2,2}$ is obtained from Fig. 7 by simple trigonometry. Using the law of cosines gives

$$\beta_{2,2} = \cos^{-1}\frac{b^2+c^2-a^2}{2bc}$$

$$= \cos^{-1}\frac{1}{2}\left\{\left[(x_{2,2}-x_{1,1})^2+(y_{2,2}-y_{1,1})^2\right]\left[(x_{2,2}-x_{2,1})^2+y_{2,2}^2\right]\right\}^{-1/2}$$

$$\left[(x_{2,2}-x_{1,1})^2+(y_{2,2}-y_{1,1})^2+(x_{2,2}-x_{2,1})^2-(x_{2,1}-x_{1,1})^2\right]$$

In this expression we have adopted the following notation: the coordinates of the point 2 on C_2 are given by $(x_{2,2}, y_{2,2})$. Thus, $(x_{2,1}, y_{2,1})$ denote the coordinates of point 1 on C_2; $(x_{1,1}, y_{1,1})$ denote the coordinates of point 1 on C_1. Clearly, the first subscript denotes the boundary (C_1 or C_2) on which the point lies while the second subscript denotes the point itself. Now, we consider the evaluation of the line integral in Eq. (16). We construct a line from point 2 on C_2 to a typical point 10 on C_1, see Fig. 7. We construct the inwardly-directed unit normal N_t to C_1 at point 10 as shown. The angle enclosed by this normal and the constructed line is the angle (n_t, r). It will prove convenient at this point to define the angle $\psi_{1,10}$, the angle included between the outwardly directed unit normal to C_1 at 10 and the x-direction. Clearly, from Fig. 7, we get:

$$(n_t, r) = \omega^{1,10}_{2,2} - \psi_{1,10}$$

wherein $\omega^{1,10}_{2,2}$ denotes the angle associated with the point 2 on C_2 (we use subscripts 2,2) between the x-direction and the line from point 2 on C_2 to point 10 on C_1. Now

$$\cos(n_t, r) = \cos\left(\omega^{1,10}_{2,2} - \psi_{1,10}\right)$$

or

$$\frac{\cos(n_t, r)}{r} = \frac{(x_{1,10} - x_{2,2})\cos\psi_{1,10} + (y_{1,10} - y_{2,2})\sin\psi_{1,10}}{(x_{1,10} - x_{2,2})^2 + (y_{1,10} - y_{2,2})^2}$$

It must be pointed out that this expression is associated only with the points 2,2 and 1,10. The integrand of the line integral can now be written as

$$\theta_{1,10} F^{1,10}_{2,2} \Delta\sigma_1$$

wherein

$$F^{1,10}_{2,2} = \frac{(x_{1,10}-x_{2,2})\cos\psi_{1,10} + (y_{1,10}-y_{2,2})\sin\psi_{1,10}}{(x_{1,10}-x_{2,2})^2 + (y_{1,10}-y_{2,2})^2}$$

We have considered only one point, 10 on the boundary C_1, but in accord with Eq. (16) we must perform a line integration over the entire boundary C_1. Thus, we must follow the procedure outlined above for point 10 on C_1 for all points on C_1 and then, and only then, can we approximate the line integral by a sum. It follows then, that Eq. (16) becomes

$$\theta_{2,2} = -2\beta_{2,2} + \pi - \frac{1}{\pi}\sum_{q=1}^{40} \theta_{1,q} F^{1,q}_{2,2} \Delta\sigma_1$$

We can generalize this result to apply to any point i on C_2, i.e.,

$$\theta_{2,i} = -2\beta_{2,i} + \pi - \frac{1}{\pi}\sum_{q=1}^{40} \theta_{1,q} F^{1,q}_{2,i} \Delta\sigma_1 \quad ; \quad (i = 2,3,4,5)$$

where

$$F^{1,j}_{2,i} = \frac{(x_{1,j} - x_{2,i})\cos\gamma_{1,j} + (y_{1,j} - y_{2,i})\sin\gamma_{1,j}}{(x_{1,j} - x_{2,i})^2 + (y_{1,j} - y_{2,i})^2}$$

$$(j = 1, 2, \cdots, 40) \qquad (17b)$$

and

$$\beta_{2,i} = \cos^{-1}\frac{1}{2}\left\{\left[(x_{2,i} - x_{1,1})^2 + (y_{2,i} - y_{1,1})^2\right]\left[(x_{2,i} - x_{2,1})^2 + y^2_{2,i}\right]\right\}^{-1/2}\left[(x_{2,i} - x_{1,1})^2 + (y_{2,i} - y_{1,1})^2 + (x_{2,i} - x_{2,1})^2 - (x_{2,1} - x_{1,1})^2\right] \qquad (17c)$$

Because of symmetry we have the following relationship

$$\theta_{i,5j+1} = \phi_{i,5j+1} = j\,\pi/4, \qquad \begin{matrix} i=1,2 \\ j=0,1,2,\ldots,7 \end{matrix}$$

Consequently, we do not require relationships such as Eq. (17), corresponding to those boundary points which lie on axes of symmetry. Thus, we have four Eqs. (17) corresponding to i = 2,3,4,5 among the following unknowns:

$$\theta_{2,2},\ \theta_{2,3},\ \theta_{2,4},\ \theta_{2,5}$$

and

$$\theta_{1,2},\ \theta_{1,3},\ \theta_{1,4},\ \theta_{1,5}$$

Clearly, four additional equations are required and these we obtain in a similar fashion from Eq. (6b). Following a procedure similar to that used in establishing Eq. (17) we obtain the following from Eq. (6b)

$$\theta_{1,i} = -2\beta_{1,i} + \frac{1}{\pi}\sum_{q=1}^{40} \theta_{2,q}\, F_{1,i}^{2,q}\, \Delta\sigma_2 - \frac{1}{\pi}\sum_{q=1}^{40} \theta_{1,q}\, F_{1,i}^{1,q}\, \Delta\sigma_1 \qquad (18a)$$

$$(i = 2,3,4,5)$$

where

$$F_{1,i}^{2,q} = \frac{(x_{2,q} - x_{1,i})\cos\gamma_{2,q} + (y_{2,q} - y_{1,i})\sin\gamma_{2,q}}{(x_{2,q} - x_{1,i})^2 + (y_{2,q} - y_{1,i})^2}$$

$$(q = 1,2,\cdots,40)$$

$$\beta_{1,i} = \cos^{-1}\frac{1}{2}\left\{\left[(x_{1,i} - x_{1,1})^2 + (y_{1,i} - y_{1,1})^2\right]\left[(x_{1,i} - x_{2,1})^2 + y_{1,i}^2\right]\right\}^{-1/2}$$

$$\left[(x_{1,i} - x_{1,1})^2 + (y_{1,i} - y_{1,1})^2 + (x_{1,i} - x_{2,1})^2 - (x_{2,1} - x_{1,1})^2\right] \qquad (18c)$$

$$F^{1,q}_{1,i} = \frac{(x_{1,q} - x_{1,i})\cos\gamma_{1,q} + (y_{1,q} - y_{1,i})\sin\gamma_{1,q}}{(x_{1,q} - x_{1,i})^2 + (y_{1,q} - y_{1,i})^2}$$

$$(q = 1, 2, \cdots, 40)$$

$$i \neq q$$

(18d)

It is important to point out that $F^{1,q}_{1,i}$ becomes indeterminate when q = i. It is necessary to evaluate the limit of Eq. (18d) when $q \to i$. Since

$$x_{1,q} = x_{1,q}(\sigma_1)$$

and

$$y_{1,q} = y_{1,q}(\sigma_1)$$

it is easy to see that:

$$\cos\gamma_{1,q} = \frac{dy_{1,q}}{d\sigma_1} = y'_{1,q}$$

$$\sin\gamma_{1,q} = -\frac{dx_{1,q}}{d\sigma_1} = -x'_{1,q}$$

Thus, using L'Hopital's Theorem:

$$F^{1,i}_{1,i} = \lim_{q\to i} F^{1,q}_{1,q} = \lim_{q\to i} \frac{(x_{1,q}-x_{1,i})y''_{1,q} - (y_{1,q}-y_{1,i})x''_{1,q}}{2(x_{1,q}-x_{1,i})x'_{1,q} + 2(y_{1,q}-y_{1,i})y'_{1,q}}$$

$$= \lim_{q\to i} \frac{x'_{1,q}\,y''_{1,q} + (x_{1,q}-x_{1,i})y'''_{1,q} - y'_{1,q}\,x''_{1,q} - (y_{1,q}-y_{1,i})x'''_{1,q}}{2x'^{2}_{1,q} + 2(x_{1,q}-x_{1,i})x''_{1,q} + 2y'^{2}_{1,q} + 2(y_{1,q}-y_{1,i})y''_{1,q}}$$

$$F^{1,i}_{1,i} = \frac{x'_{1,i}\,y''_{1,i} - y'_{1,i}\,x''_{1,i}}{2(x'^{2}_{1,i} + y'^{2}_{1,i})} = \frac{1}{2\rho_{1,i}}$$

(18e)

Where $\rho_{1,i}$ is the radius of curvature at point i on C_1.* Equations (17a) and (18a) constitute a system of eight unknown arguments which we must now solve. Clearly, we obtain eight equations because of the number of points chosen on the boundaries of B_z. If we subdivide C_1 and C_2 into 2pN segments where N is any integer we shall obtain 2(N - 1) equations analogous Eqs. (17) and (18) in 2(N - 1) unknown arguments; viz.,

$$\theta_{2,i} = -2\beta_{2,i} + \pi - \frac{1}{\pi}\sum_{q=1}^{2pN} \theta_{1,q}\,F^{1,q}_{2,i}\,\Delta\sigma_1$$

$$(i = 2,3,4,\cdots N) \qquad (19a)$$

*See Ref. (5), p. 151.

$$\theta_{1,i} = -2\beta_{1,i} + \frac{1}{\pi}\sum_{q=1}^{2pN} \theta_{2,q} F_{1,i}^{2,q} \Delta\sigma_2 - \frac{1}{\pi}\sum_{q=1}^{2pN} \theta_{1,q} F_{1,i}^{1,q} \Delta\sigma_1$$

$$(i = 2,3,4,\cdots,N) \qquad (19b)$$

wherein the quantities F are given by Eqs. (17b), (18b) and (18d) except that j and q range from 1 to 2pN. In the specific problem considered, Fig. 7, N = 5 so we obtained eight equations.

APPLICATIONS OF THE NUMERICAL PROCEDURE

For a given domain B_z with p-axes of symmetry it is necessary to select first the number 2pN of segments along C_1 and C_2 or in essence to select the integer value N. For

$$0 \leq \emptyset_i < 2\pi \qquad (i = 1,2)$$

we shall have 2pN points. The coordinates of the points along C_2 are very easily determined to be

$$x_{2,k} = R \cos (k-1) \frac{\pi}{N.p} \qquad : k = 1,2,\ldots 2pN$$

$$y_{2,k} = R \sin (k-1) \frac{\pi}{N.p} \qquad : k = 1,2,\ldots 2pN$$

where R is the radius of C_2. The angle $\psi_{2,k}$ is easily seen to be

$$\psi_{2,k} = (k-1) \frac{\pi}{N.p} \qquad : k = 1,2,\ldots 2pN$$

The coordinates $(x_{1,q}, y_{1,q})$ of points on C_1 constitute given data since the boundary C_1 is given in the form of an analytical expression relating the coordinate variables of points on C_1, or in the form of a table expressing the same relationship or in some other equivalent form. Thus, $x_{1,q}$ and $y_{1,q}$ for the preselected points on C_1 are determined in a suitable manner depending upon how C_1 is defined. The determination of the angles $\psi_{1,q}$ can be done graphically or analytically. An exact determination of $\psi_{1,q}$ will require the knowledge of

$$y = y(x)$$

or the equivalent formulation

$$y_1 = y_1\ (\sigma_1)$$

$$x_1 = x_1\ (\sigma_1)$$

Thus:

$$\psi = \tan^{-1}\left[-\frac{dx_1}{d\sigma_1} \Big/ \frac{dy_1}{d\sigma_1}\right]$$

If N is large, an accurate determination can be done by replacing

$$\frac{dx_1}{d\sigma_1} \Big/ \frac{dy_1}{d\sigma_1}$$

with

$$\frac{\Delta x_1 / \Delta \sigma_1}{\Delta y_1 / \Delta \sigma_1} = \frac{x_{1,q} - x_{1,q-1}}{y_{1,q} - y_{1,q-1}}$$

As a numerical example let us consider the domain B_z, shown, in Fig. 8, with a square inner boundary (C_1) and a circular outer boundary (C_2). It is of interest to point out that the web fraction w for this domain is 0.75. We begin by taking N = 5 so the 2pN = 40 since there are four axes of symmetry. The next step is to evaluate the coordinates, $(x_{1,i}, y_{1,i})$ and $(x_{2,i}, y_{2,i})$ of the pre-selected points on the boundaries C_1 and C_2, respectively, as explained in the preceding paragraphs. Next, the angles

$\psi_{1,i}$ and $\psi_{2,i}$ are determined analytically or graphically as appropriate. With the above as input information Eqs. (19) were solved on an IBM 7090 digital computer for the eight unknown angles; viz.,

$$\theta_{i,j} = \theta_{i,j}(\phi_{i,j}); \qquad \begin{matrix} i = 1,2 \\ j = 2,3, \ldots 8 \end{matrix}$$

The functional relations $\theta_i = \theta_i(\phi_{i,j})$ are shown in Figs. 9 and 10. We notice that θ_1 is negative for $0 < \theta_1 < 13°$. This is not admissible for a one to one correspondence between points on γ_1 and C_1; for one value of θ we have two different values of ϕ. Clearly the number of divisions taken is not enough for an accurate determination of the relations $\theta_i = \theta_i(\phi_i)$.

Taking $2pN = 80$ $(N = 10)$ the situation improves considerably and for $2pN = 160 (N = 20)$ θ_1 is positive for all values of ϕ_1. Comparing Figures 9 and 10 we notice that the functional relation $\theta_1 = \theta_1(\phi_1)$ is very sensitive to the number of intervals taken along C_1. However $\theta_2 = \theta_2(\phi_2)$ does not change in such a drastic manner when the number of divisions is increased. This result is not unexpected since the numerical procedure requires solution of Eqs. (6b) and (14). In Eq. (14) it is necessary to integrate once numerically while in Eq. (6b) it is necessary to integrate twice by numerical procedures. Therefore we expect a greater accumulation of error in Eq. (6b).

Figure 11 shows the functional relations $\theta_i = \theta_i\ (\phi_1)$ for a domain B_z shown in Fig. 12. The web fraction w is equal to 0.91.

A domain with an hexagonal inner boundary is shown in Figure 13. The calculated values of θ_i as functions of ϕ_i are shown in Figure 14. for 2pN = 120 (p = 6 in this case).

It is one of the objectives of this investigation to consider the influence of the web fraction on the relation $\theta_i = \theta_i\ (\phi_i)$. Comparing $\theta_2 = \theta_2\ (\phi_2)$ (Figure 10) corresponding to w = 0.75 and $\theta_2 = \theta_2\ (\phi_2)$ (Figure 11) corresponding to w = 0.91 we immediately notice the fact that as w decreases, the functional relation between θ_2 and ϕ_2 approaches $\theta_2 = \phi_2$. This conclusion agrees with Wilson[1] who developed a very interesting method for obtaining the mapping function when the web fraction is relatively small. This is further illustrated for the case of a star-shaped perforation (Figure 15). As shown in Figure 16 for the configuration of Figure 15, as the web fraction w decreases the functional relation $\theta_2 = \theta_2\ (\phi_2)$ approaches the expression $\theta_2 = \phi_2$.

THE MAPPING FUNCTION

Concerning the transformation of an annulus onto an arbitrary doubly connected region, the following theorem is known [4]:

"Any doubly connected region can be transformed, conformally and with reciprocal single - valuedness, into an annulus with the radii of its bounding circumferences finite or infinite."

We are concerned with a domain B_z wherein the outer boundary C_2 is circular and B_z has p-axes of symmetry. We denote the radii of the circumferences γ_1 and γ_2 corresponding to C_1 and C_2 by ρ_1 and ρ_2, respectively. Once we specify which of the boundary curves of the region must pass to the outer and which to the inner circumference of the annulus the ratio ρ_1/ρ_2 will be fully defined. Evaluation of this ratio constitutes one of the difficult problems of the theory of conformal transformation [4]. Clearly we can always take ρ_1 or ρ_2 equal to unity and the unknown will be ρ_2 or ρ_1 respectively.

The transformation function which maps B_z onto B_ξ can be determined in a straightforward manner, using Eqs. (4b) and (1) once the functional relations $\theta_i = \theta_i(\phi_i)$ are known. In this manner

$$\xi = f(z) = e^{F(z)}$$

can be found. However for convenience in applications (mathematical theory of elasticity, vibrations, etc.) it is important to know the function which maps an annulus onto the given shape; i.e., $z = z(\xi)$. Clearly if $\xi = \xi(z)$ is known, in principle, one could invert this relation to

obtain the above. However it is more convenient to determine $z = z(\xi)$ directly once both integral equations are solved.

In general the function which maps B_ξ onto B_z can be expanded in a Laurent series [4]; i.e.,

$$z = \sum_{j=-\infty}^{+\infty} a_{1+jp}\, \xi^{1+jp} \tag{20a}$$

From a practical point of view, if the series above is truncated at a finite number of terms, a sufficiently accurate transformation will result. Thus, we obtain

$$z = \sum_{j=-q}^{+s} a_{1+jp}\, \xi^{1+jp}$$

The unknowns, now are the coefficients a_i.

Let us take for convenience $\rho_1 = 1$. We know that $\rho_2 > 1$ and we will assume that it is a known value for the time being. Separating Eq. (20b) into real and imaginary parts we obtain:

$$\begin{aligned} Re\, z = X = a_{1-qp}\rho^{1-qp}\cos(1-qp)\theta + \\ +\cdots + a_{1-p}\rho^{1-p}\cos(1-p)\theta + a_1\rho\cos\theta + \\ +\cdots + a_{1+sp}\rho^{1+sp}\cos(1+sp)\theta \end{aligned} \tag{21b}$$

$$\text{Im } z = y = a_{1-qp}\rho^{1-qp}\sin(1-qp)\theta +$$

$$+\cdots+ a_{1-p}\rho^{1-p}\sin(1-p)\theta + a_1\rho\sin\theta +$$

$$+\cdots+ a_{1+sp}\rho^{1+sp}\sin(1+sp)\theta \qquad (21b)$$

Equations (21) will now be used in developing a system of linear algebraic equations with the a_i's as the unknowns. The domains B_z and B_ξ are known since we have assumed, for the time being, that ρ_2 is known and, consequently, corresponding to each point on C_1 and C_2 we can write Eqs. (21) with only the a_i's as unknown. This is true since we have already established the procedure by which the points on C_1 and C_2 can be related to their image points on γ_1 and γ_2, respectively. In Eqs. (21) we have $(q + S + 1)$ unknown coefficients $a_i (q, S \geq 1)$. Therefore, we require $(q + S + 1)$ equations. At the points $\theta = 0$ and π/p Eqs. (21) degenerate to a single equation. On the other hand corresponding to any other point Eqs. (21) are independent and not degenerate. Whether we choose to include one or both of Eqs. (21) in the system which we shall solve for the a_i's is unimportant. It is only essential that we finally obtain a system of $(q + S + 1)$ equations.

For points on C_1, $\rho = \rho_1$ and $\theta_1 = \theta_1(\phi_1)$. Taking any point with coordinates $(x_{1,j}, y_{1,j})$ the image point in the ξ-plane will be

located on the unit circle γ_1 and its coordinates will be given by

$$\xi_{1,j} = \rho_1 e^{i\theta_{1,j}} = \cos\theta_{1,j} + i\sin\theta_{1,j}$$

The value of $\theta_{1,j}$ will be known from $\theta_{1,j} = f(\tan^{-1} y_{1,j}/x_{1,j})$ since the integral equations (6b) and (14) have been solved. The same procedure is used for points on C_2. We can take any arbitrary number of points on C_1; say n and m points on C_2 for which $\rho = \rho_2$. Thus it will prove convenient to rewrite Eq. (20b) in the following form

$$z = \sum_{j=0}^{n-1} a_{1-jp}\,\xi^{1-jp} + \sum_{j=1}^{m} a_{1+jp}\,\xi^{1+jp} \qquad (22a)$$

In this form we have (n + m) coefficients to determine. Using Eqs. (21) for n - points on C_1 ($\rho = 1$) and m - points on C_2 ($\rho = \rho_2$) we obtain a linear system of equations in the (n + m) coeficients of the truncated series (22a). Solving this linear system of equations the coefficients are found and the approximate mapping function is known.

Let us return to the determination of ρ_2. Methods are available in the literature to find ρ_2. However those methods are very difficult to apply in practical problems. The following direct approach is suggested: We take (n + m) points on C_1 and C_2 and we write Eq. (22a) in the following form:

$$Z = \sum_{j=0}^{n-1} a_{1-jp}\, \xi^{1-jp} + \sum_{j=1}^{m-1} a_{1+jp}\, \xi^{1+jp} \qquad (22b)$$

Proceeding as previously explained we write down (n + m) equations where now the unknowns are (n + m - 1) coefficients and ρ_2. However we observe now that we have n - linear equations in the unknown coefficients and m - nonlinear equations in the unknown coefficients and ρ_2. It is quite convenient to obtain the unknowns by using a method of successive approximations without solving the nonlinear system of equations directly. The procedure is the following. As a first approximation to the mapping function which maps the annulus B_ξ onto the domain B_z we determine the mapping function which maps the outside of the unit circle in the ξ -plane onto the outside of C_1 in the Z-plane; i.e., we write

$$Z^{(0)} = \sum_{j=0}^{n-1} a^{(0)}_{1-jp}\, \xi^{1-jp} \quad ; \quad \xi = \rho e^{i\theta} \qquad (23a)$$

The coefficients $a^{(0)}_{1-jp}$ are calculated from a system of n-linear equations obtained from n-points on C_1. For $\rho = 1$, Eq. (23a) maps the unit circle γ_1 in the ξ-plane onto the contour C_1 in the Z-plane. For $\rho_2 >> 1$

Eq. (23a) maps circles in the ξ-plane onto approximate circles in the z-plane. If the radius of C_2 is R, we can obtain $\rho_2^{(1)}$ by requiring that:

$$R = a_1^{(o)} \rho_2^{(1)} \quad \therefore \rho_2^{(1)} = R/a_1^{(o)}$$

In order to obtain a second approximation we write (n + m - 1) equations in the (n + m - 1) coefficients; namely,

$$z^{(1)} = \sum_{j=0}^{n-1} a_{1-jp}^{(1)} \xi^{1-jp} + \sum_{j=1}^{m-1} a_{1+jp}^{(1)} \xi^{1+jp} \qquad (23b)$$

considering n-points on C_1 and (m - 1) points on C_2. We exclude from this system the equation corresponding to the point $\theta_{2,m} = \phi_{2,m} = \pi/p$ which has coordinates $(x_{2,m}; y_{2,m})$ in the Z-plane. The system of (n + m - 1) equation is solved for the (n + m - 1) unknowns $a_i^{(1)}$ using $\rho_2 = \rho_2^{(1)}$. Corresponding to the point $\phi_{2,m} = \pi/p$ we have

$$x_{2,m}^{(1)} + i y_{2,m}^{(1)} = \sum_{j=0}^{n-1} a_{1-jp}^{(1)} \xi^{1-jp} + \sum_{j=0}^{m-1} a_{1+jp}^{(1)} \xi^{1+jp} \qquad (23c)$$

wherein $\xi = \rho_2^{(1)} e^{i\pi/p}$. Separating real and imaginary parts we calculate $x_{2,m}^{(1)}$ and $y_{2,m}^{(1)}$. In general

$$x_{2,m}^{(1)} \neq x_{2,m}$$

$$y_{2,m}^{(1)} \neq y_{2,m}$$

We must now evaluate the next approximation, $\rho_2^{(2)}$, to ρ_2. We follow a procedure similar to that used in arriving at $\rho_2^{(1)}$. We write Eq. (23b) for $\theta_{2,m} = \phi_{2,m} = \pi/p$ = ;i.e.,

$$\left|z^{(1)}\right| = \cdots + a_{1-2p}^{(1)} \left|\xi_2\right|^{1-2p} - a_{1-p}^{(1)} \left|\xi_2\right|^{1-p}$$

$$+ a_1^{(1)} \left|\xi_2\right| - a_{1+p}^{(1)} \left|\xi_2\right|^{1+p} + a_{1+2p}^{(1)} \left|\xi_2\right|^{1+2p} + \cdots$$

It turns out that the predominant term in this sequence is the one involving the first power of $\left|\xi_2\right|$ while the other terms more or less cancel each other. Consequently, we take the following as a second approximation to ρ_2 :

$$\rho_2^{(2)} = R/a_1^{(1)}$$

Using this new approximation we calculate a new mapping function as before. If it turns out that

$$x^{(2)}_{2,m} = x_{2,m}$$

$$y^{(2)}_{2,m} = y_{2,m}$$

to within some arbitrarily pre-selected accuracy, the procedure is completed and the mapping function determined. If the above criterion is not satisfied, the next approximation is determined by linear interpolation on a plot of $\rho_2^{(i)}$ versus $R^{(i)}$ wherein:

$$R^{(i)} = \left\{ \left[x^{(i)}_{2,m} \right]^2 + \left[y^{(i)}_{2,m} \right]^2 \right\}^{1/2}$$

In essence, $R^{(i)}$ denotes the i - th approximation to R. From this plot we select the next approximation as that value of ρ_2 which corresponds to R. The procedure is repeated until the criterion is satisfied to any desired accuracy. Once the mapping function is determined to the desired accuracy we can plot the boundaries of the resulting doubly connected region and compare them with the given boundaries C_1 and C_2. Both sets of curves will have at least (n + m) points in common. As the number of points chosed increases indefinitely we can assume that both sets of curves will coincide. For practical reasons it is desirable to carefully

select the collocation points so as to maintain a minimum number of equations for an optimum approximation of the curve. The procedure outlined above depends on the requirement that the mapping function transforms the circular annulus point-by-point onto the desired domain. The procedure may be extended to include conditions on the curvature of the given contours as well. This statement will be illustrated in a subsequent application.

FURTHER APPLICATIONS

We will consider first a simple example which will serve as an illustration of the method of successive approximations. Let B_z be the domain shown in Figure 17. In this application it is our objective to illustrate only the successive approximation procedure developed in the previous section. The $\theta - \phi$ relationship implied in the data given below was independently developed using the method established earlier for this purpose. The following conditions will be used in order to find the function which maps B_ξ in the ξ-plane onto B_z in the z-plane:

Inner Boundary (C_1)

a. At point A $(\phi_{1,A} = 0^\circ;\ \theta_{1,A} = 0^\circ)$; Re z = 1.00

b. At point A the radius of curvature is infinite

c. At point B $(\phi_{1,B} = 4^\circ;\ \theta_{1,B} = 15^\circ)$; Im z = 0.067

d. At point C $(\phi_{1,C} = 45^\circ;\ \theta_{1,C} = 45^\circ)$; Im z = 0.283

Outer Boundary (C_2)

e. At point D $(\phi_{2,D} = 0^\circ;\ \theta_{2,D} = 0^\circ)$; Re z = R = 1.243

f. At point E $(\phi_{2,E} = 45^\circ;\ \theta_{2,E} = 45^\circ)$; Re z = R cos 45° = 0.879

Eq. (22b) becomes:

$$z = \sum_{j=0}^{3} a_{1-4j}\, \xi^{1-4j} + a_5\, \xi^5 \qquad (24)$$

wherein the unknowns are:

$$a_1,\ a_{-3},\ a_{-7},\ a_{-11},\ a_5 \text{ and } \rho_2$$

Using conditions a, b*, c and d we proceed to calculate the coefficients of

$$z^{(o)} = \sum_{j=o}^{3} a_{1-4j}^{(o)} \xi^{1-4j} \tag{25a}$$

Solving the resulting four linear equations we obtain:

$$z^{(o)} = 0.7789\xi + 0.2965\,\xi^{-3} - 0.0789\xi^{-7} + 0.0034\xi^{-11} \tag{25b}$$

As a first approximation to ρ_2 we take

$$\rho_2 = \rho_2^{(1)} = \frac{1.243}{a_1^{(o)}} = 1.60$$

and we determine the coefficients of

$$z^{(1)} = \sum_{j=o}^{3} a_{1-jp}^{(1)} \xi^{1-4j} + a_5^{(1)} \xi^5$$

---

*Condition (b) reduces to $a_1^{(o)} + 9a_{-3}^{(o)} + 49a_{-7}^{(o)} + 121\,a_{-11}^{(o)} = 0$ (See (5), p. 151).

from a system of five equations using conditions a, b, c, d and e. The function obtained is:

$$z^{(1)} = 0.78836\xi + 0.2997\xi^{-3} - 0.08836\xi^{-7} + 0.00871\xi^{-11} - 0.0084\xi^{5} \tag{25c}$$

For $\xi = 1.60e^{i\,\pi/4}$ we obtain

$$x^{(1)}_{2,E} = y^{(1)}_{2,E} = 0.865$$

We determine a new value of $\rho_2^{(2)}$; viz.

$$\rho_2^{(2)} = R/a_1^{(1)} = 1.57$$

and repeating the same procedure we find

$$x^{(2)}_{2,E} = y^{(2)}_{2,E} = 0.905$$

By linear interpolation we obtain $\rho_2^{(3)} = 1.58$ and for $\xi = 1.58\ e^{i\,\pi/4}$

$$x^{(3)}_{2,E} = y^{(3)}_{2,E} = 0.879$$

The final expression for the mapping function is:

$$z = 0.78726\ \xi + 0.2993\ \xi^{-3} - 0.08726\ \xi^{-7} + 0.0081\ \xi^{-11} - 0.007415\xi^{+5} \tag{25d}$$

The maximum error in the mapping of C_2 is less than one per cent (see

TABLE 1). It is important to point out that addition of one single term ($a_5\ \xi^5$) to Eq. (25a) reduces the error ten times. Using additional points on C_2, the mapping of the outer circle could be improved even more.

As a second example let us consider the domain B_z, shown in Figure 8 with a square inner boundary (C_1) and a circular outer boundary (C_2). It is convenient to consider rounded corners instead of ideal angular points. The conditions used for calculating the mapping function are obtained from Figures 9 and 10 where the $\theta_i = \theta_i(\phi_i)$ functional relations are plotted. (See TABLE II)

Following the procedure previously explained we find $\rho_2 = 1.5912$ and the corresponding mapping function is:

$$z = 5.9037737\xi - 0.9956698\ \xi^{-3} + 0.08597233\ \xi^{-7} - 0.0249356\xi^{-11} +$$

$$+ 0.009366175\ \xi^{-15} - 0.003723699\ \xi^{-19} + 0.000958236\xi^{-23} +$$

$$+ 0.0241344\ \xi^{5} + 0.00005452\ \xi^{9} \qquad (26)$$

The maximum error for C_1 is of the order of 0.002 per cent and for C_2 is 0.02 per cent (See TABLE III).

It is important to point out that without including point 2 on C_2 the error for C_2 is of the order of 0.1 per cent. It should be remarked that following Wilson's approach [1] the error for C_2 would be of the order of ± 5 per cent.

Now we consider the domain B_z, shown in Figure 12. The web fraction in this case is equal to 0.91. Using the relations plotted in Figure 11 we select the conditions shown in TABLE IV. Following the procedure previously explained we find $\rho_2 = 1.275$ and the corresponding mapping function:

$$z = 5.9712317\,\xi - 1.1506136\,\xi^{-3} + 0.01595684\,\xi^{-7} - 0.01573124\,\xi^{-11} + \\ + 0.00365151\,\xi^{-15} - 0.0003575\,\xi^{-19} - 0.000217676\,\xi^{-23} + 0.00008544\,\xi^{-27} + \\ + 0.1665126\,\xi^{+5} + 0.0088086\,\xi^{+9} \qquad (27)$$

The maximum error in the mapping of C_2 is of the order of +1 per cent and for C_1 is 0.002 per cent. (See TABLE V). The approach followed in [1] would yield an error of ± 10 per cent.

For the domain B_z shown in Figure 13 ($\theta_i = \theta_i\,(\phi_i)$ is shown in Figure 14, seven points were selected on C_1 and two points on C_2. (See TABLE VI). The procedure of successive approximations yields $\rho_2 = 1.1823$ and the mapping function is:

$$z = 5.3248059\,\xi - 0.4027524\,\xi^{-5} + 0.0308024\,\xi^{-11} - 0.0088643\,\xi^{-16} + \\ +0.002342932\,\xi^{-21} - 0.000247309\,\xi^{-26} - 0.00011216\,\xi^{-31} + 0.054006\,\xi^{+6} \qquad (28)$$

The error in both contours is practically zero (TABLE VII). It should be pointed out that following the approach described in [1] the error would be approximately ± 3 per cent when mapping C_2.

CONCLUSIONS

It is shown in the present investigation that the system of two integral equations obtained by Kantorovitch and Muratov for the conformal mapping of an arbitrary, finite, doubly connected region onto a circular annulus simplifies considerably when the configuration has one or more axes of symmetry and one of the boundaries is a circle. Once the correspondence between boundary points is established the function which maps the annulus B_ξ in the ξ-plane onto the given domain B_z in the z-plane is obtained by a procedure of successive approximations. The method is illustrated in several cases where the web fraction is close to one. The numerical procedure has been performed only for regions with an outer circular boundary as this was the main goal of this investigation. If the configuration has p-axes of symmetry and the inner (rather than the outer) boundary is a circle one could find the correspondence between points by solving the integral equations (6a) and (15) and obtain the mapping function using the method of successive approximations described in Chapter IV. Configurations of this type are of practical interest also. Consider, for example, the graphite brick of a gas-cooled nuclear reactor which is a long bar of square cross section with a concentric circular perforation [7]. The collocation technique used in [7], when solving Laplace's equation, yields considerable error when the web fraction is greater that 0.50. The method of conformal mapping presented in this investigation does not have that limitation and the solution will be much more accurate. For other configurations, such as doubly connected regions

bounded by two concentric rectangles, it will be necessary to solve Eqs. (6) to obtain the point correspondence between domains but the mapping function may be determined as shown in Chapter IV. Configurations of this type are of great interest in certain problems of microwave theory [8]

REFERENCES

1. Wilson, H. B., "A Method of Conformal Mapping and the Determination of Stresses in Solid Propellant Rocket Granins." Report No. S-38, Rohm and Haas Co., Alabama. (Also Doctoral dissertation of H. B. Wilson at the Department of Theoretical and Applied Mechanics. University of Illinois, Urbana, Illinois) 1963.

2. Arango, R., "Simple Method of Conformal Transformation of a Solid Propellant Rocket Motor Cross-Section." Master's Thesis, Mechanics Division, Catholic University, Washington, D. C. (1964).

3. Kantorovitch, L. V. and V. Muratov, "Conformal Mapping of Simply and Multiply Connected Regions." Edited by Smirnov, "Works of the Scientific Research Institute of Mathematics and Mechanics," Leningrad State University Moscow, Leningrad, 1937.

4. Kantorovitch, L. V. and A. N. Krylov, "Approximate Methods of Higher Analysis." Interscience Publishers, Inc., 1958, New York.

5. Granville, W. A., "Elements of Differential and Integral Calculus." Ginn and Co., New York, 1941.

6. Bergman, Stefan, "Partial Differential Equations, Advanced Topics." Brown University, Summer Session, 1941.

7. Hockney, R. W., " A Solution of Laplace's Equation for a Round Hole in a Square Peg." Journal of the Society of Industrial and Applied Mathematics, Vol. 12, No. 1, March, 1964.

8. Cruzan, O. R. and R. V. Garver, "Characteristic Impedance of Rectangular Coaxial Transmission Lines." IEEE Transactions on Microwave Theory and Techniques. Number 5. September, 1964.

APPENDIX

Let us evaluate the expression

$$f(\sigma_2) = 0 \qquad \frac{\theta_2(\sigma_2)\cos(n_t, r)}{r} \quad d\sigma_2$$

when Z is a point Z_{c2} on C_2. From Figure 3 we obtain:

$$\frac{\cos(n_t, r)}{r} d\sigma_2 = d\omega$$

since $d\sigma_2 \cdot \cos(n_t, r)$ is the projection of $d\sigma_2$ on the normal to the direction of r. Thus

$$f(\sigma_2) = \oint_{C_2} \theta_2(\sigma_2)\, d\omega$$

Adding and substraction the argument corresponding to the point z which will be defined as θ_z, we have

$$f(\sigma_2) = \oint_{C_2} [\theta_2(\sigma_2) - \theta_z]\, d\omega + \oint_{C_2} \theta_z \cdot d\omega$$

However

$$\oint_{C_2} \theta_z \, dw = \theta_z \int_0^{2\pi} dw = 2\pi \cdot \theta_z$$

(see Figure 4 - a)

Accordingly:

$$f(\sigma_2) = \oint_{C_2} [\theta_2(\sigma_2) - \theta_z] \, dw + 2\pi \cdot \theta_z$$

Let us now evaluate $f(\sigma_2)$ when z is a point Z_{c2} (see Figure 4b). The integral $\oint \theta_z dw$ becomes

$$\oint \theta_z \, dw \Big|_{z = z_{C_2}} = \oint \theta_2(z_{C_2}) \, dw$$

$$= \theta_2(z_{C_2}) \int_{w_0}^{w_0 + \pi} dw$$

$$= \pi \theta_2(z_{C_2})$$

Finally

$$f(\sigma_2)\Big|_{z = z_{C_2}} = \oint_{C_2} \frac{\theta_2(\sigma_2)\cos(n_t, r)}{r} \, d\sigma_2 + \pi \theta_2(\sigma_2)$$

TABLE I

Inner Boundary (C_1)					Outer Boundary (C_2)	
Coordinates of the given curve		Calculated coordinates using Eq. (25d)				
$x_{1,i}$	$y_{1,i}$	$x_{1,i}$	$y_{1,i}$	$\theta_{1,i}$	$\theta_{2,i}$	$\lvert z_{2,i} \rvert$
1.00	0.000	1.00	0.000	0°	0°	1.243
1.00	0.030	0.999	0.031	5°	5°	1.245
1.00	0.060	0.995	0.061	12°	12°	1.251
0.98	0.067	0.984	0.067	15°	15°	1.253
0.94	0.060	0.940	0.061	21°	21°	1.257
0.86	0.050	0.863	0.051	26°	26°	1.257
0.75	0.060	0.713	0.058	32°	32°	1.252
0.60	0.090	0.585	0.090	36°	36°	1.248
0.44	0.160	0.447	0.156	40°	40°	1.245
0.283	0.283	0.283	0.283	45°	45°	1.243

TABLE II

Inner Boundary (C_1)					Outer Boundary (C_2)				
Point	$\phi_{1,i}$	$\theta_{1,i}$	$z_{1,i}$		Point	$\phi_{2,i}$	$\theta_{2,i}$	$z_{2,i}$	
			$x_{1,i}$	$y_{1,i}$				$x_{2,i}$	$y_{2,i}$
1	0°	0°	5.00		1	0	0	9.40	
2	12°	5°	5.00		2	25°	22°	8.449	
3	26.6°	15°	5.00		3	45°	45°	6.647	
4	32.5°	20°	5.00						
5	41°	30°	5.00						
6	44.2°	40°	5.00						
7	45°	45°		4.95					

TABLE III

	Inner Boundary (C_1)		Outer Boundary (C_2)		
θ (degrees)	$z_{1,i}$		$z_{2,i}$		
	$x_{1,i}$	$y_{1,i}$	$x_{2,i}$	$y_{2,i}$	$\lvert z_{2,i} \rvert$
0	4.99995	0.0000	9.39988	0.0000	9.39988
2	4.99994	0.299774	9.39151	0.39678	9.39989
4	4.999934	0.598611	9.36652	0.79151	9.39990
6	4.999977	0.89553	9.32529	1.18220	9.39993
8	5.00008	1.189519	9.26843	1.56694	9.39995
10	5.00002	1.47959	9.19677	1.94399	9.39998
12	5.00017	1.76487	9.11129	2.31180	9.40000
14	5.00004	2.0446	9.01315	2.66899	9.40002
16	4.99983	2.31796	8.90357	3.01449	9.40004
18	4.99973	2.58423	8.78384	3.34743	9.40006
20	4.99992	2.84242	8.65524	3.66721	9.40008
22	5.00039	3.09145	8.51902	3.97351	9.40013
24	5.00093	3.33032	8.37636	4.26623	9.40020
26	5.00113	3.55823	8.22826	4.54551	9.40032
28	5.00076	3.77470	8.07567	4.81169	9.40047
30	4.99992	3.97932	7.91930	5.06529	9.40067
32	4.99918	4.17135	7.75969	5.30698	9.40089
34	4.99927	4.34923	7.59717	5.53756	9.40115
36	5.00041	4.51038	7.43188	7.75791	9.40140
38	5.00157	4.65142	7.26379	5.96895	9.40165
40	4.99992	4.76897	7.09263	6.17166	9.40185
42	4.99074	4.86069	6.91800	6.36702	9.40200
44	4.96817	4.92634	6.73934	6.55595	9.40208
45	4.94999	4.94999	6.64828	6.64828	9.40209

TABLE IV

Inner Boundary (C_1)					Outer Boundary (C_2)				
Point	$\phi_{1,i}$	$\theta_{1,i}$	$z_{1,i}$		Point	$\phi_{2,i}$	$\theta_{2,i}$	$z_{2,i}$	
			$x_{1,i}$	$y_{1,i}$				$x_{2,i}$	$y_{2,i}$
1	0°	0°	5.00		1	0	0°	7.70	
2	12°	5°	5.00		2	31.5°	22°	6.565	
3	26.6°	15°	5.00		3	45°	45°	5.444	
4	32.5°	20°	5.00						
5	41°	30°	5.00						
6	44.2°	40°	5.00						
7	45°	45°		4.95					

TABLE V

	Inner Boundary (C_1)		Outer Boundary (C_2)		
	$z_{1,i}$		$z_{2,i}$		
θ(degrees)	$x_{1,i}$	$y_{1,i}$	$x_{2,i}$	$y_{2,i}$	$\lvert z_{2,i} \rvert$
0	4.9994	0.0000	7.6996	0.0000	7.6996
3	4.9993	0.5403	7.6683	0.6656	7.697
6	4.9993	1.0706	7.5774	1.3103	7.6898
9	4.9993	1.5817	7.4354	1.9156	7.6782
12	4.9992	2.0658	7.2551	2.4676	7.6632
15	4.9993	2.5169	7.0513	2.9579	7.647
18	4.9994	2.9312	6.8391	3.3844	7.6307
21	4.9993	3.3068	6.6313	3.7503	7.618
24	4.9990	3.6435	6.4369	4.0627	7.612
27	4.9988	3.9430	6.2610	4.3309	7.613
30	4.9997	4.2068	6.1040	4.5647	7.622
33	5.0025	4.4343	5.9626	4.7724	7.637
36	5.0054	4.6234	5.8314	4.9603	7.656
39	5.0033	4.7719	5.7039	5.1324	7.6731
42	4.9878	4.8796	5.5742	5.291	7.685
45	4.9494	4.9494	5.4376	5.4376	7.689

TABLE VI

Inner Boundary (C_1)					Outer Boundary (C_2)				
Point	$\phi_{1,i}$	$\theta_{1,i}$	$z_{1,i}$ $x_{1,i}$	$y_{1,i}$	Point	$\phi_{2,i}$	$\theta_{2,i}$	$z_{2,1}$ $x_{2,i}$	$y_{2,i}$
1	0°	0°	5.00		1	0°	0°	6.30	
2	6°	5°	5.00		2	30°	30°		4.202
3	13°	10°	5.00						
4	19°	15°	5.00						
5	24°	20°	5.00						
6	27°	25°	5.00						
7	30°	30°	4.95						

TABLE VII

Inner Boundary (C_1)			Outer Boundary (C_2)		
	$z_{1,i}$		$z_{2,i}$		
θ(degrees)	$x_{1,i}$	$y_{1,i}$	$x_{2,i}$	$y_{2,i}$	$\lvert z_{2,i} \rvert$
0	4.9999	0.0000	6.2999	0.000	6.300
3	5.0000	0.39055	6.2851	0.4348	6.300
6	4.9999	0.7730	6.2417	0.8579	6.300
9	4.9999	1.1402	6.1736	1.2589	6.300
12	5.0000	1.4854	6.0862	1.6295	6.300
15	4.9999	1.8037	5.9862	1.9645	6.300
18	4.9995	2.0923	5.8799	2.2619	6.300
21	5.0005	2.3479	5.7726	2.5232	6.2999
24	5.0014	2.5635	5.6669	2.7531	6.300
27	4.9908	2.7324	5.5627	2.9590	6.300
30	4.9499	2.8578	5.4567	3.1505	6.300

ACKNOWLEDGMENT

The research was carried out under the supervision and guidance of Professor J. H. Baltrukonis.

The author acknowledges with gratitude the cooperation of Kevin B. Casey and Gerald Smith who programmed the numerical solution of the problem under investigation and to Miss Sara McCormack who typed the manuscript.

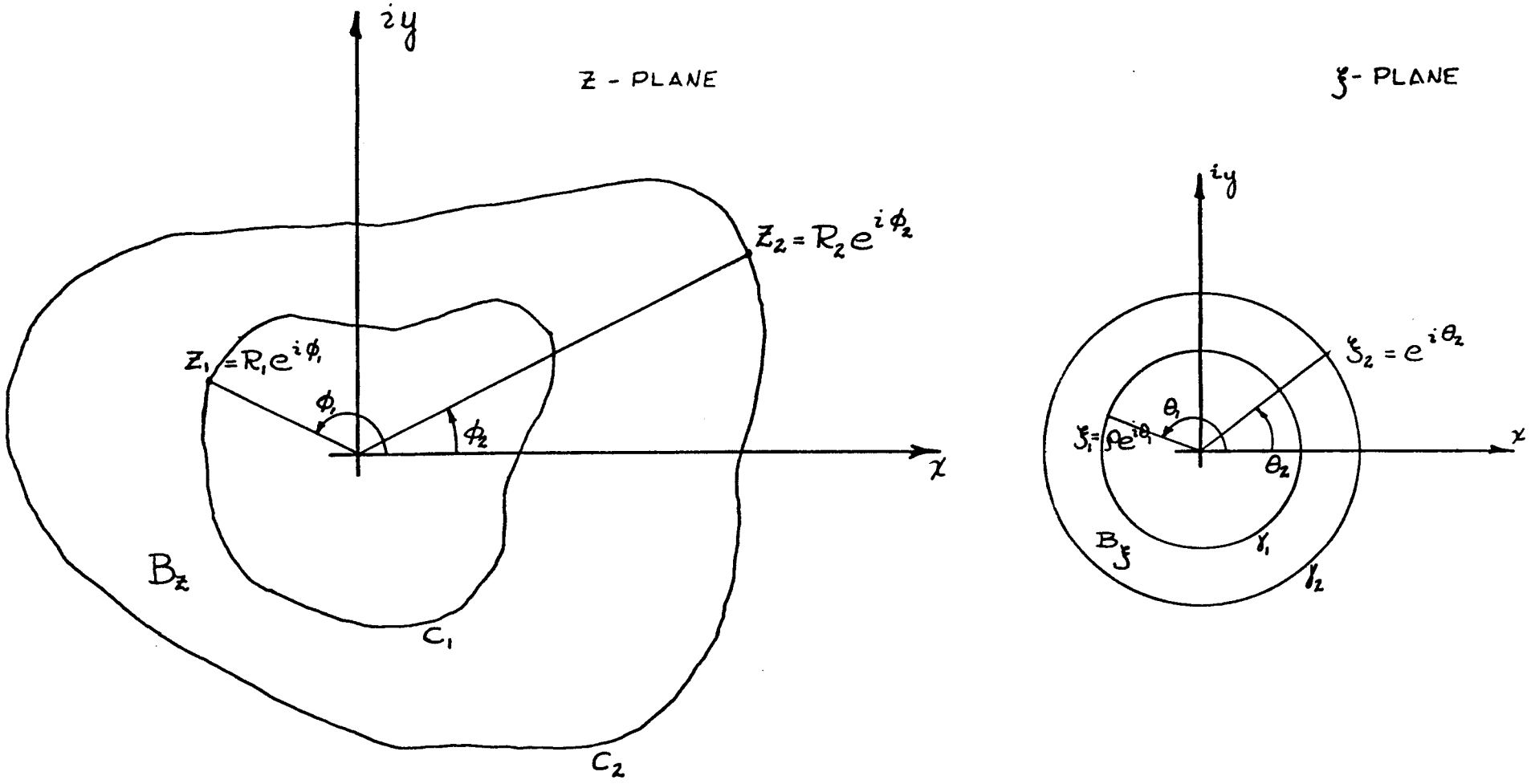
iy
Z - PLANE
$Z_2 = R_2 e^{i\phi_2}$
$Z_1 = R_1 e^{i\phi_1}$
ϕ_1
ϕ_2
x
B_z
C_1
C_2
ξ- PLANE
iy
$\xi_2 = e^{i\theta_2}$
$\xi_1 = \rho e^{i\theta_1}$
θ_1
θ_2
x
B_ξ
γ_1
γ_2

FIGURE 1

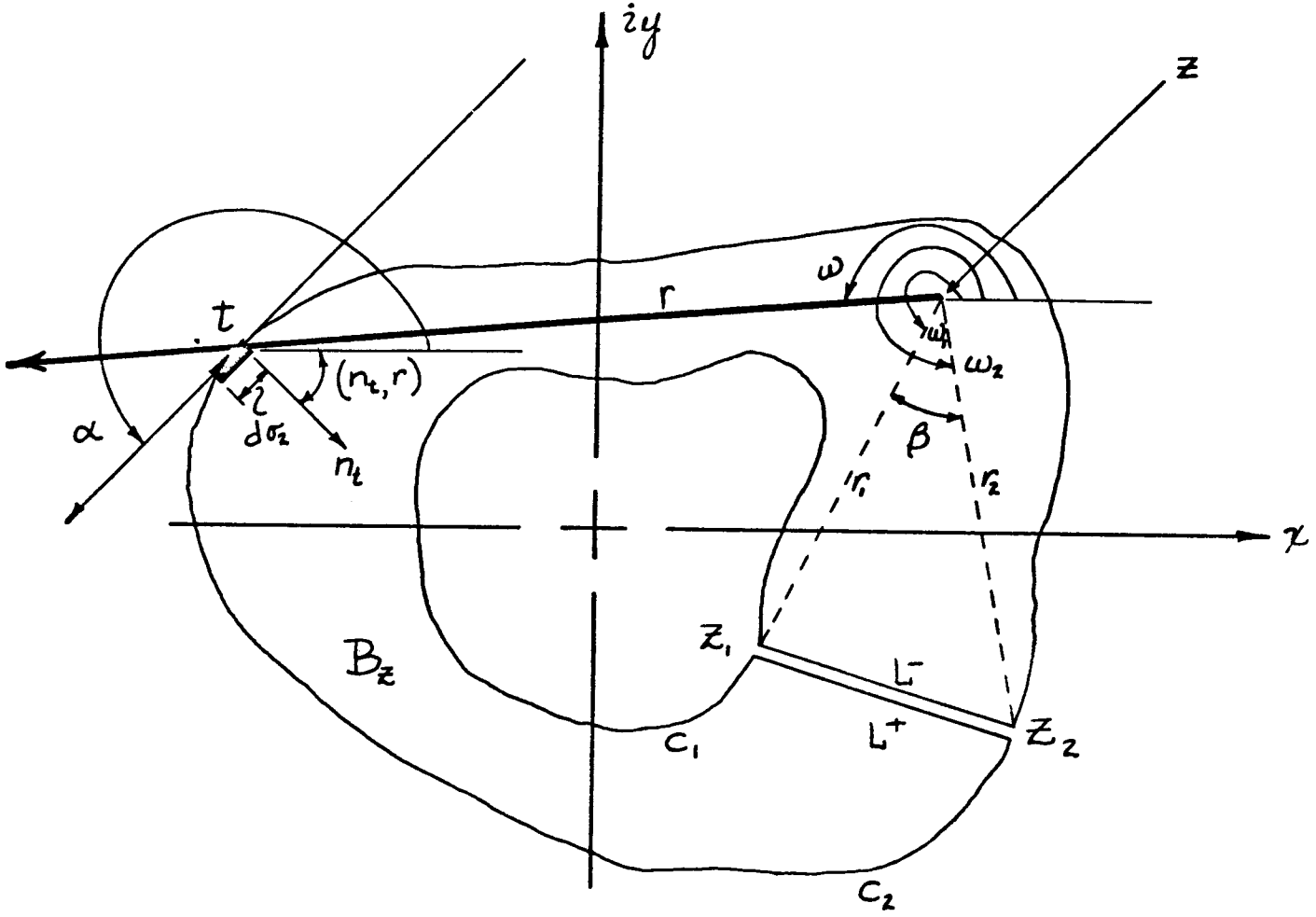

FIGURE 2

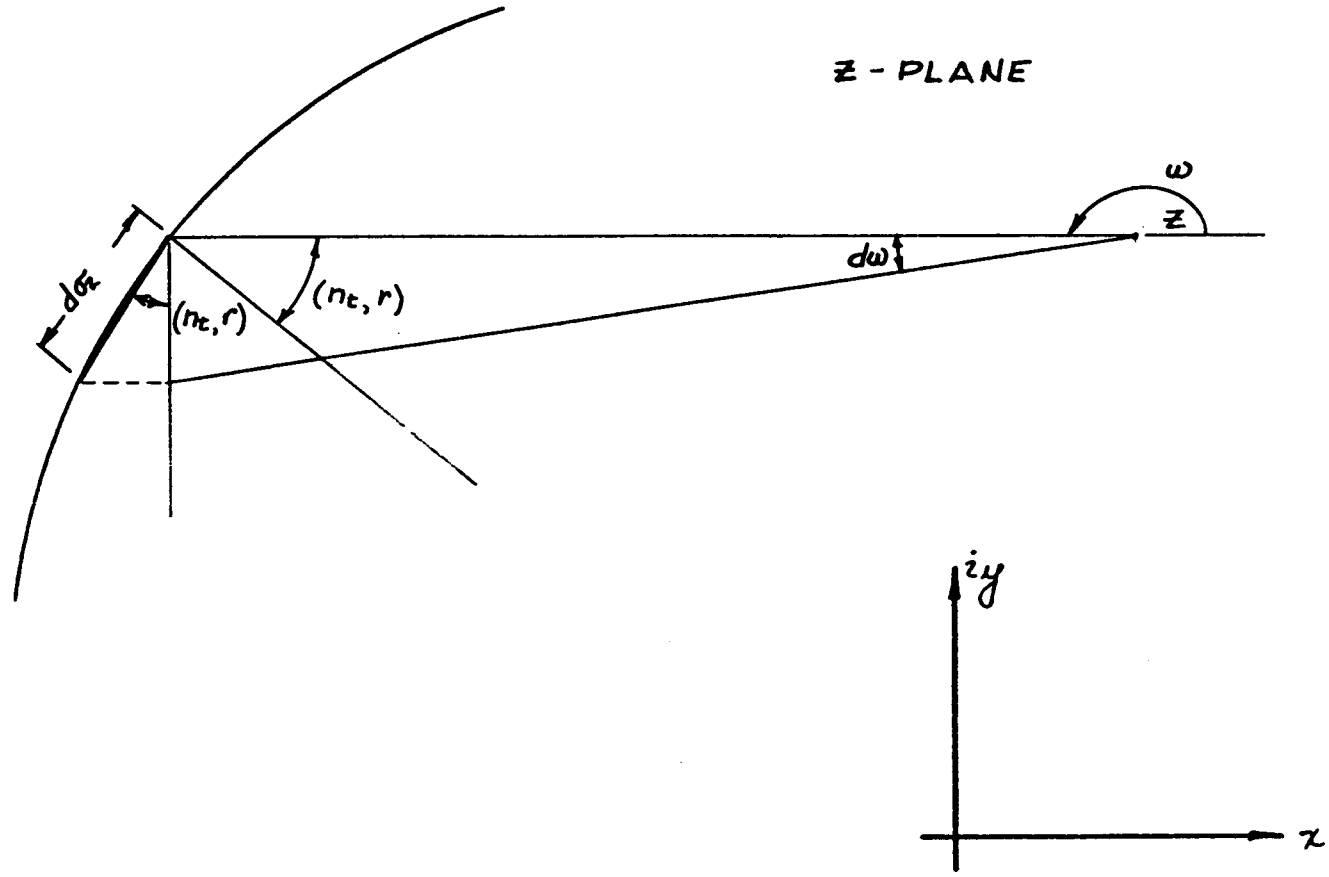

FIGURE 3

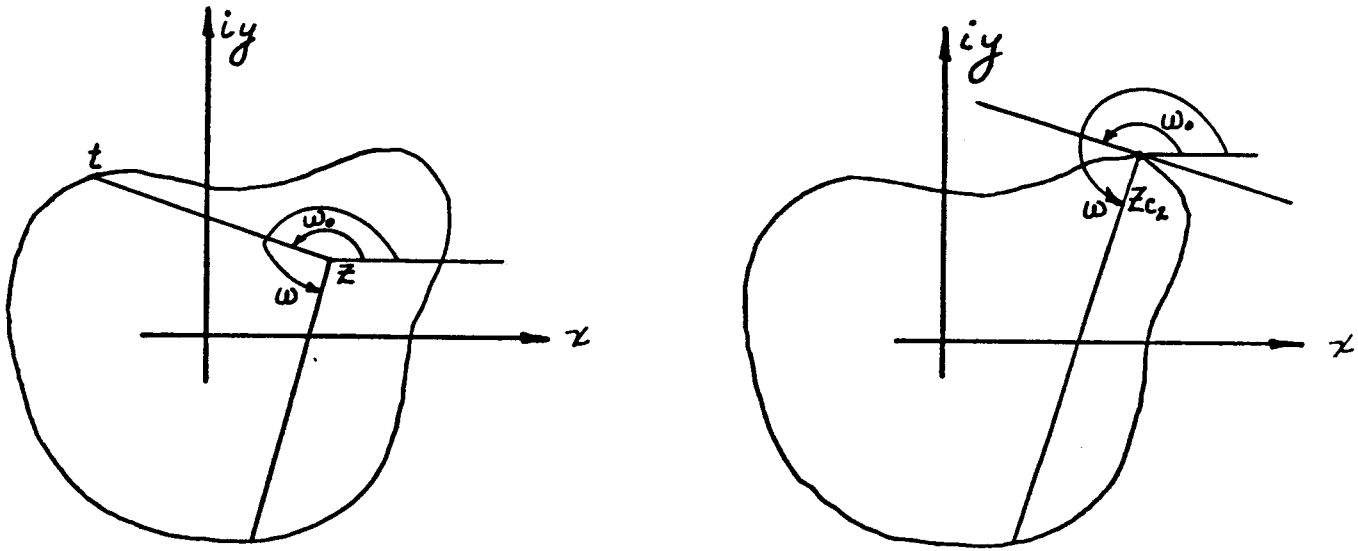

FIGURE 4

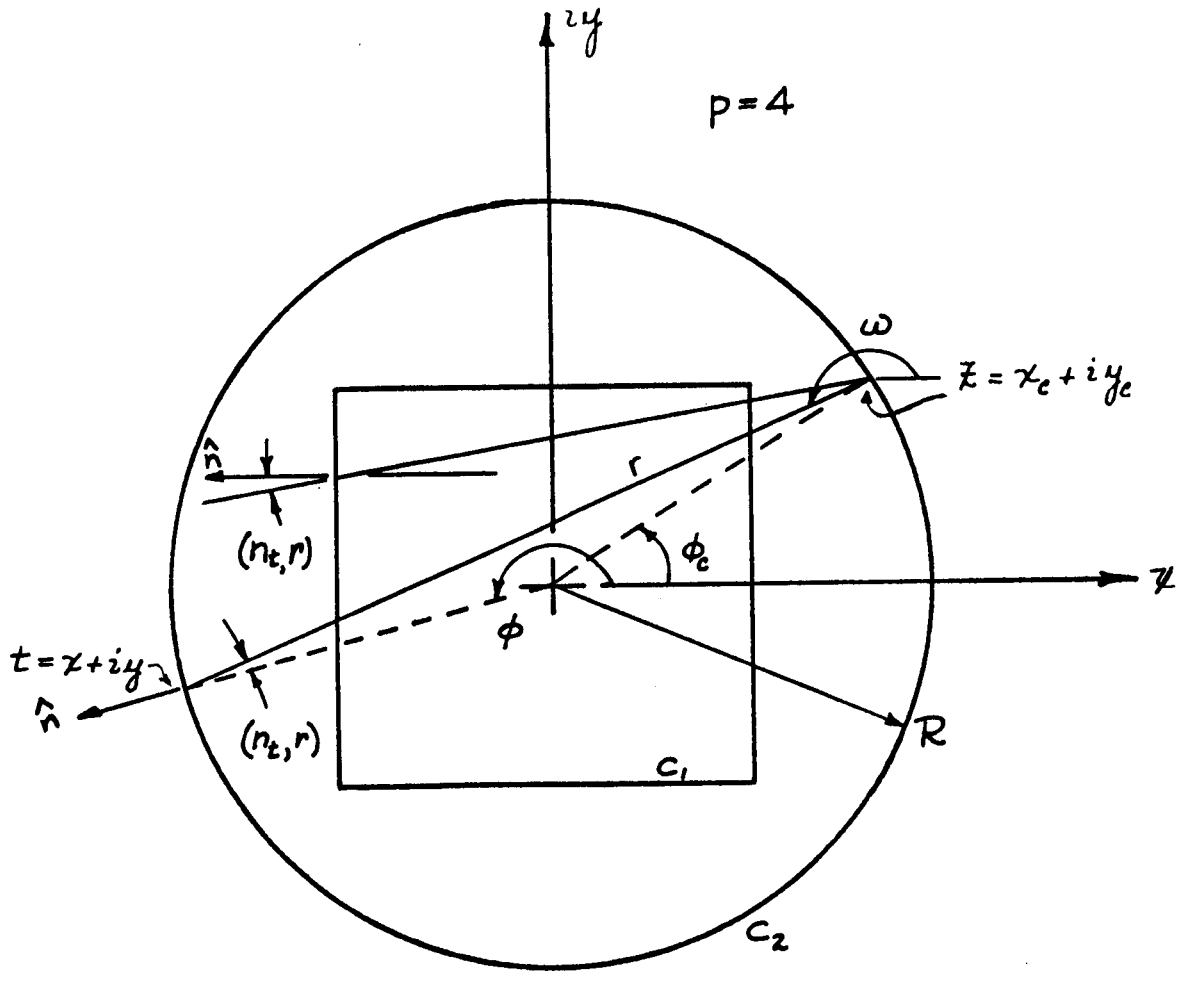

FIGURE 5

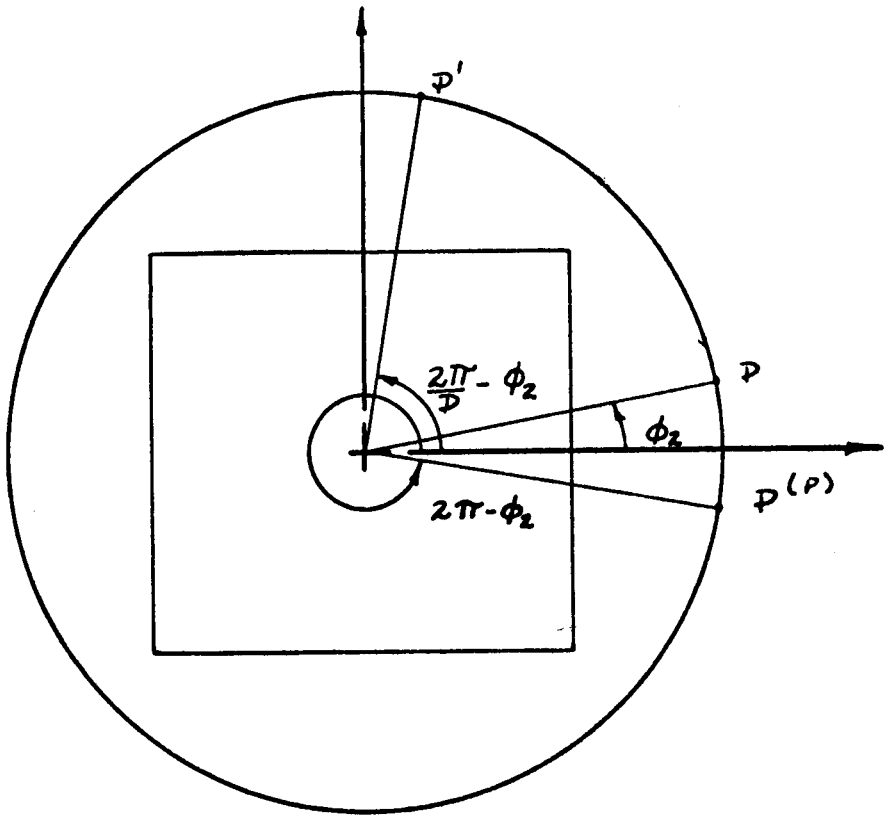

FIGURE 6

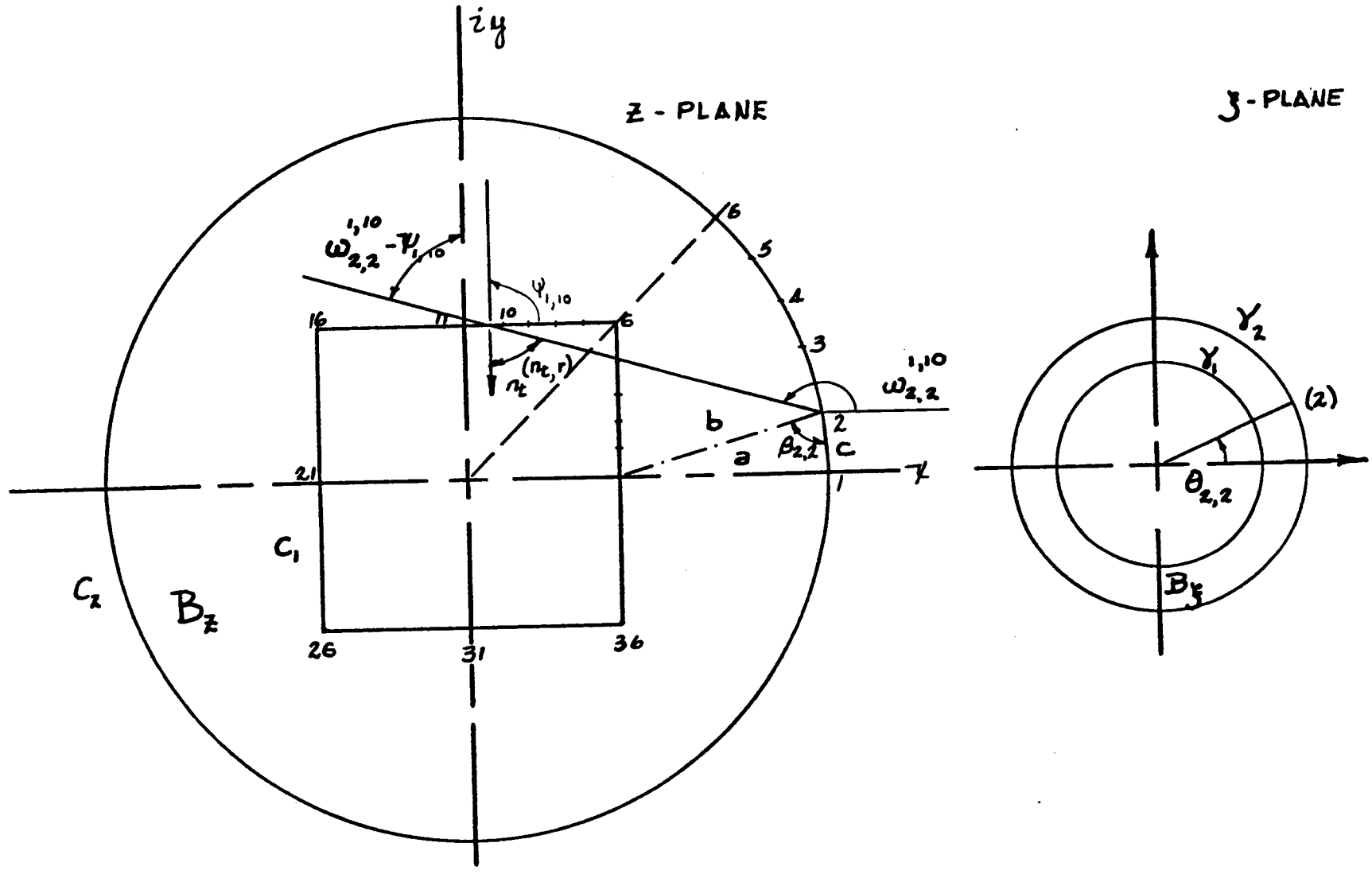
iy
Z - PLANE
ζ - PLANE
$\omega_{2,2}^{1,10} - \psi_{1,10}$
$\psi_{1,10}$
$\omega_{2,2}^{1,10}$
(n_t, r)
n_t
b
a
c
$\beta_{2,1}$
C_2
B_z
C_1
γ_2
γ_1
(2)
$\theta_{2,2}$
B_ζ
1
2
3
4
5
6
10
11
16
21
26
31
36

FIGURE 7

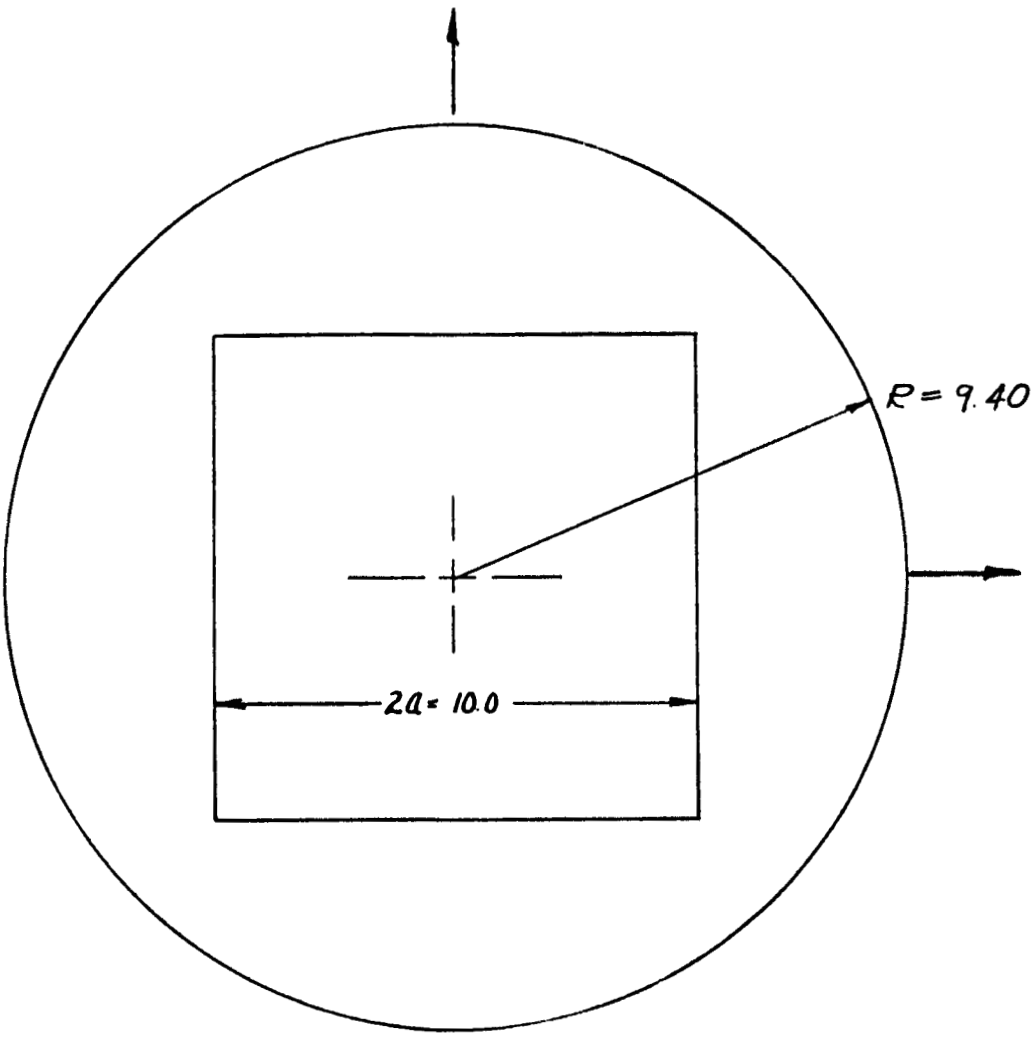

W = 0.75

FIGURE 8

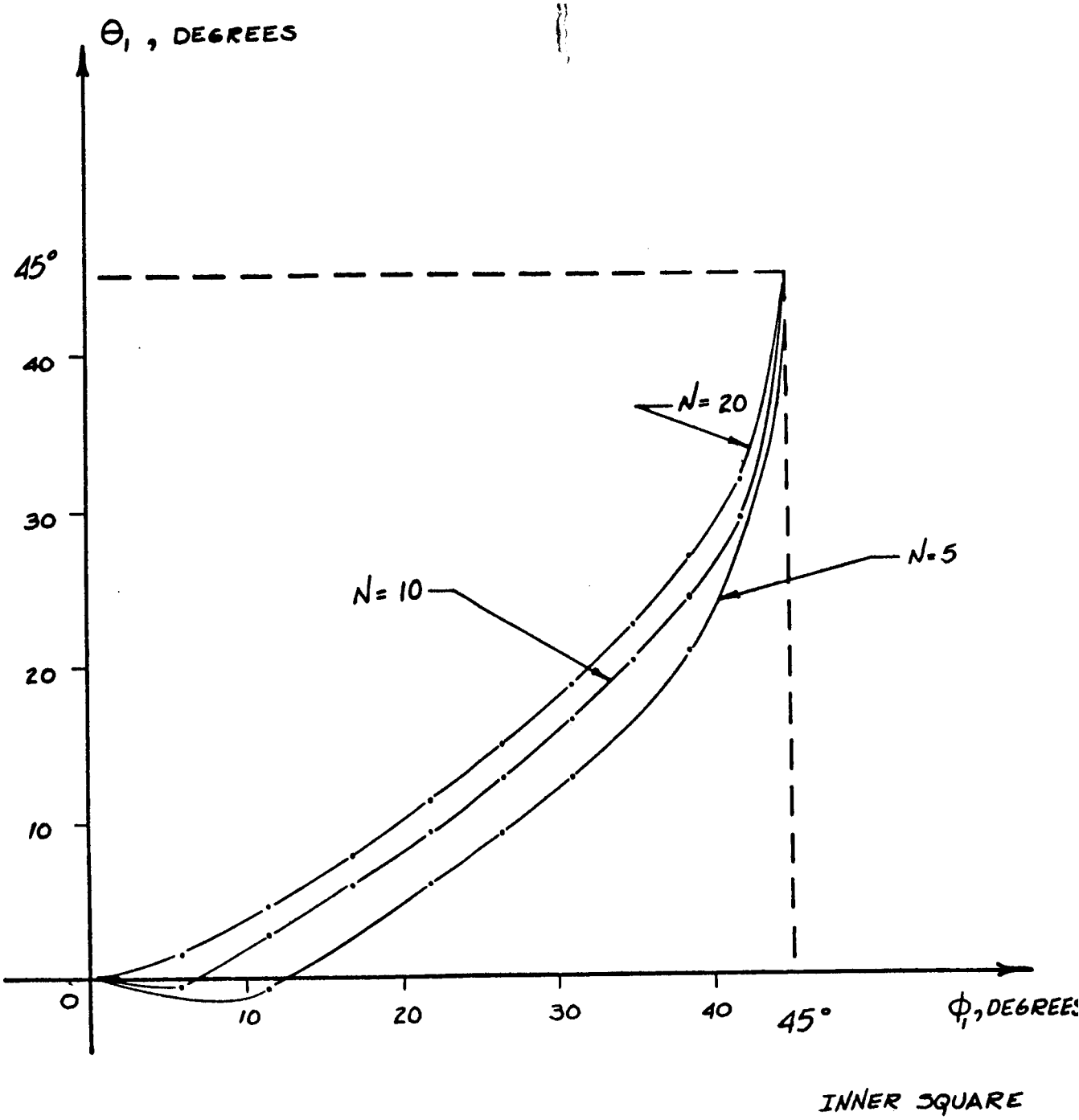
θ1 , DEGREES
45°
40
30
20
10
0
10
20
30
40
45°
φ1, DEGREES
N= 20
N= 10
N=5
INNER SQUARE

FIGURE 9

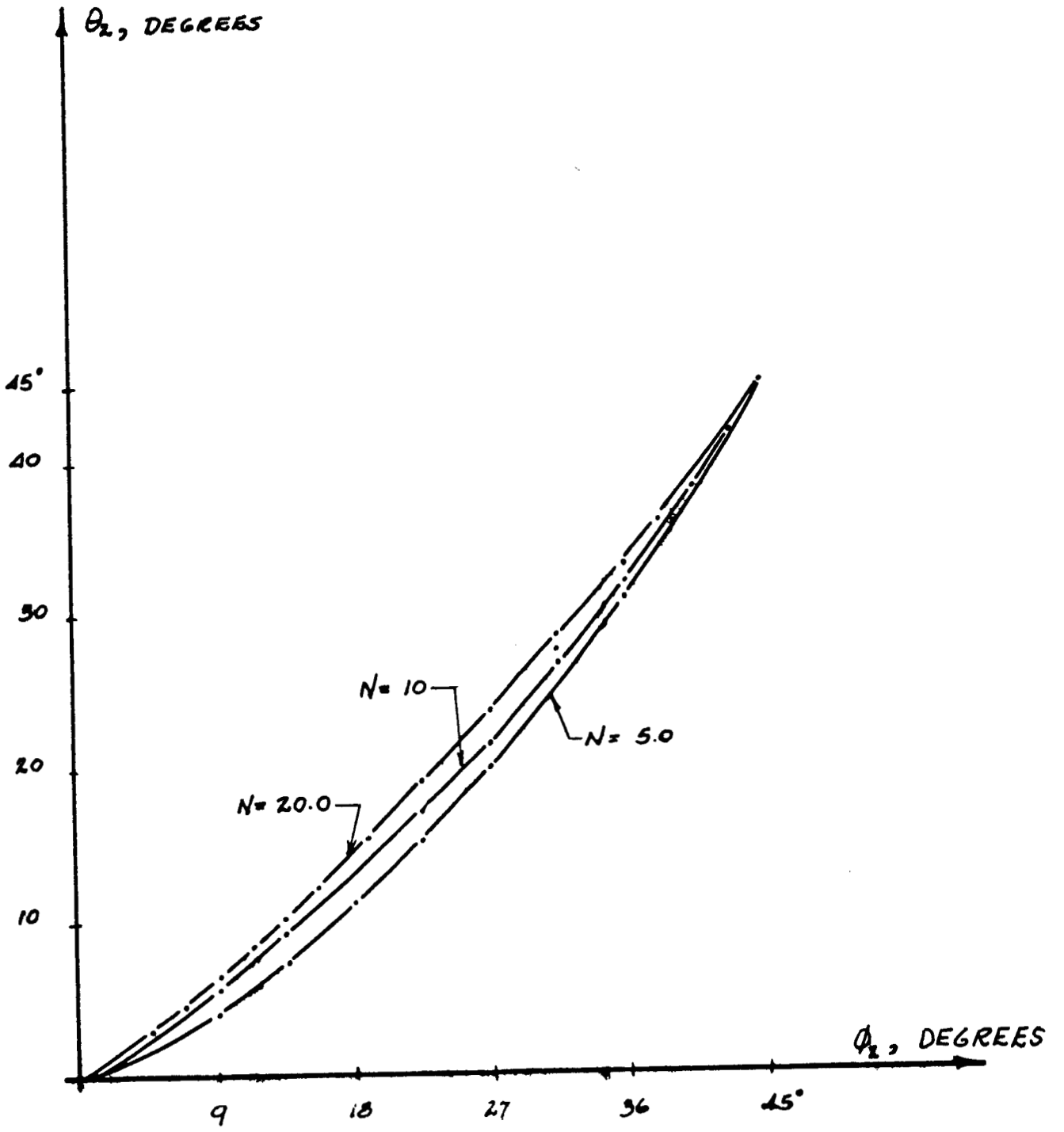

FIGURE 10

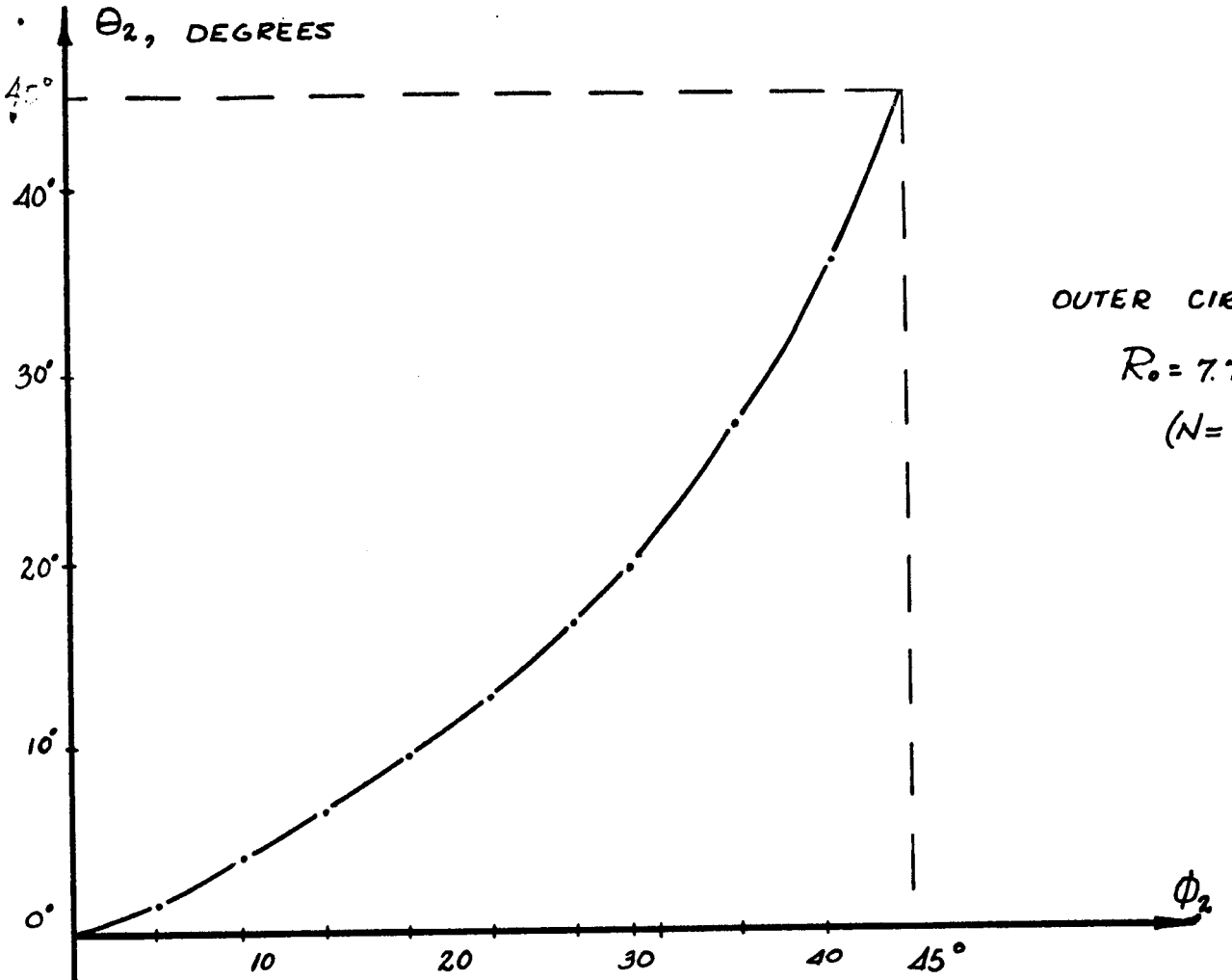
θ_2, DEGREES
45°
40°
30°
20°
10°
0°
10
20
30
40
45°
ϕ_2
OUTER CIRCLE
$R_o = 7.70$
(N = 20)

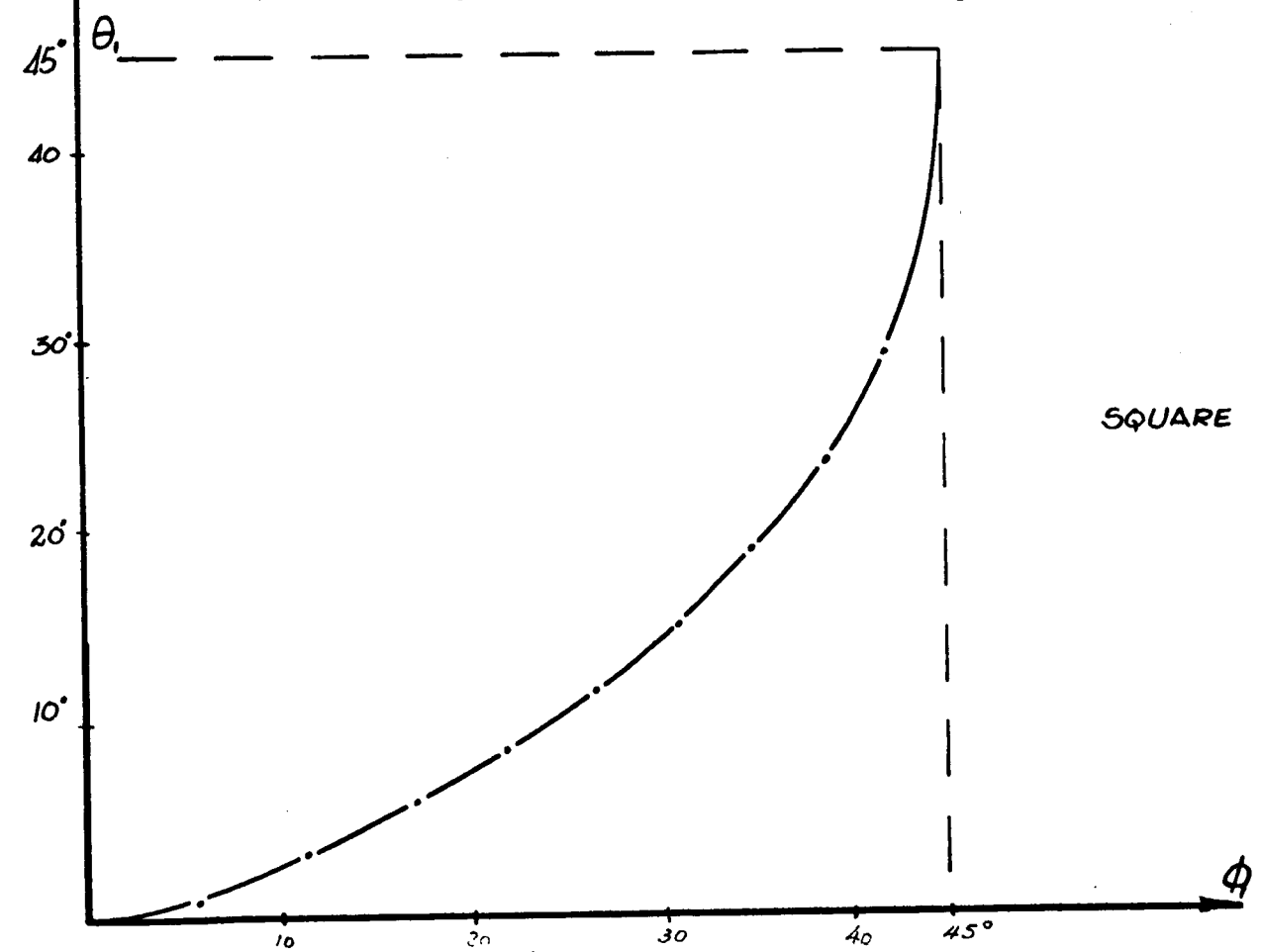
θ_1
45°
40
30°
20°
10°
10
30
40
45°
ϕ
SQUARE

FIGURE 11

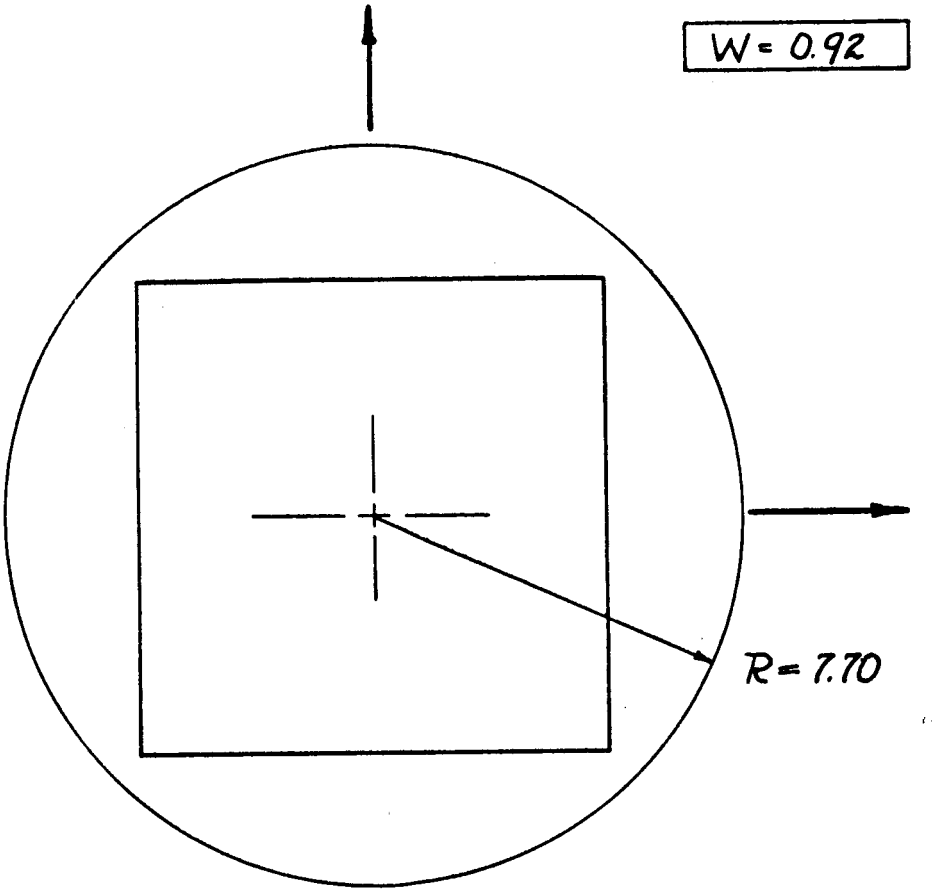

FIGURE 12

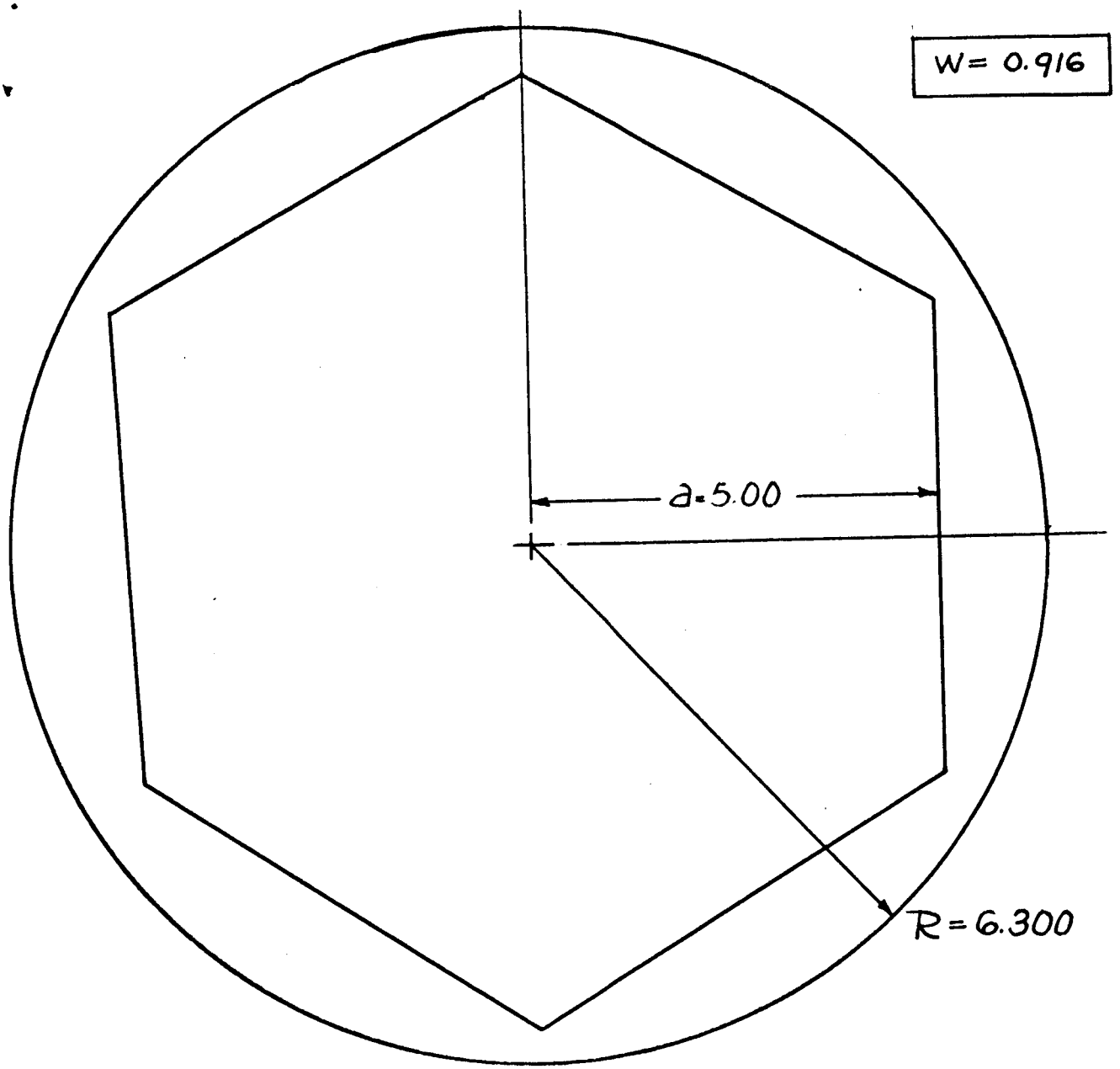

FIGURE 13

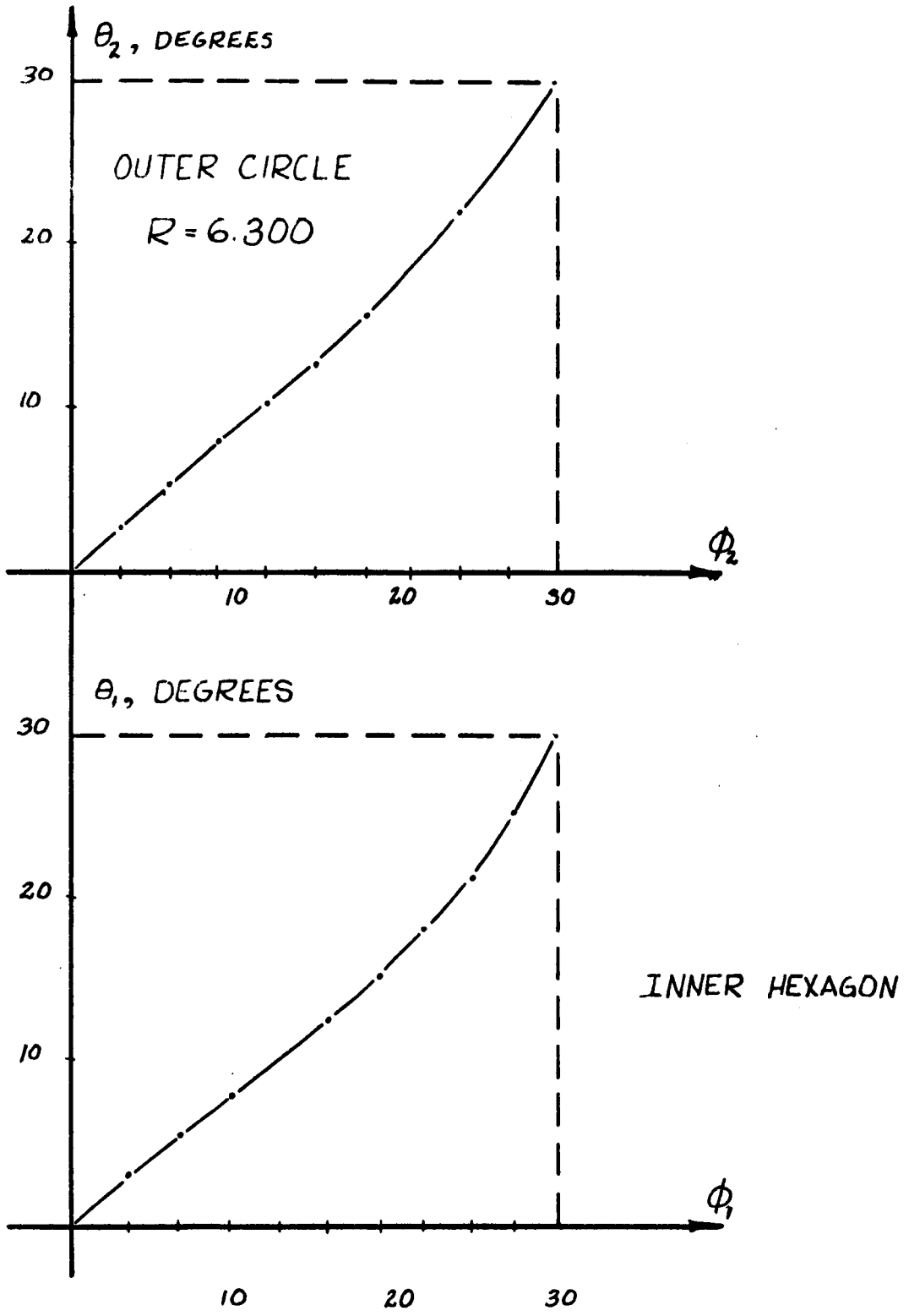
θ2, DEGREES
30
20
10
OUTER CIRCLE
R = 6.300
Φ2
10
20
30
θ1, DEGREES
30
20
10
INNER HEXAGON
Φ1
10
20
30

FIGURE 14

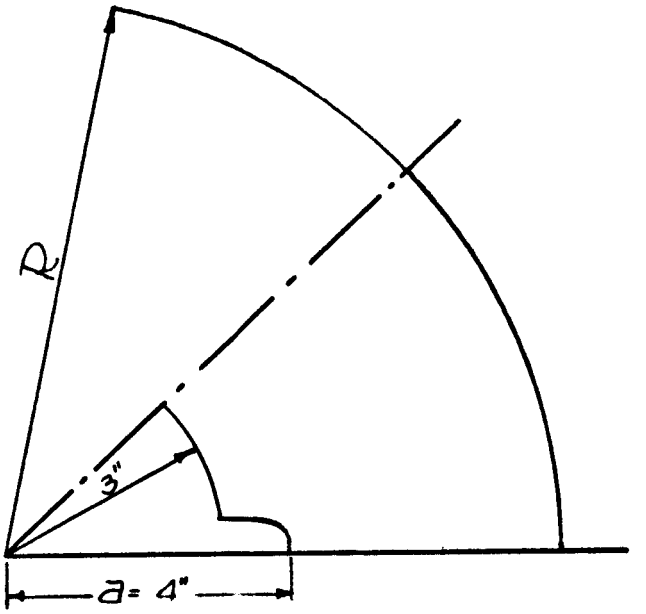

WEB FRACTION $W = a/R$

FIGURE 15

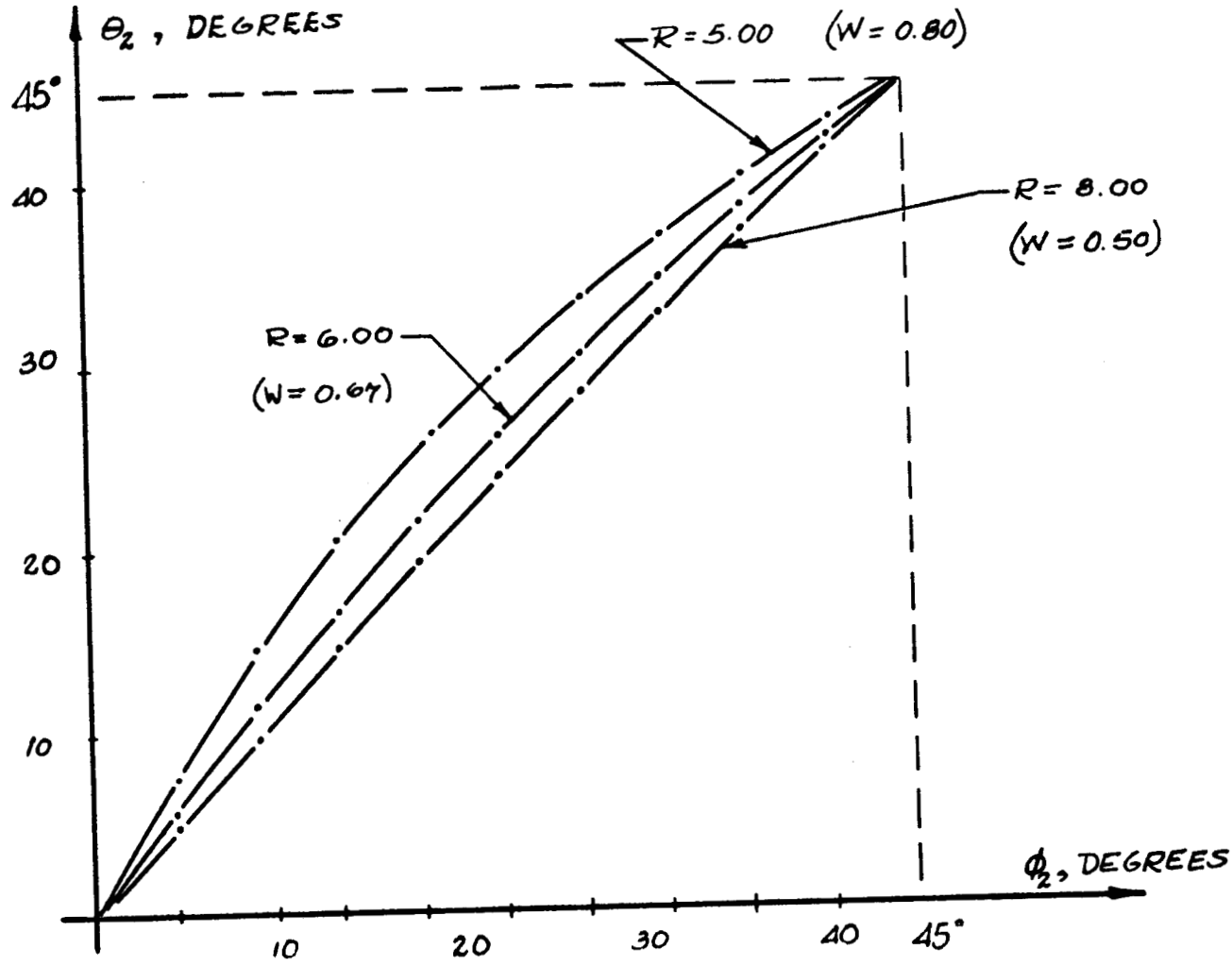
θ_2, DEGREES
45°
40
30
20
10
R = 5.00 (W = 0.80)
R = 8.00
(W = 0.50)
R = 6.00
(W = 0.67)
ϕ_2, DEGREES
10
20
30
40
45°

FIGURE 16

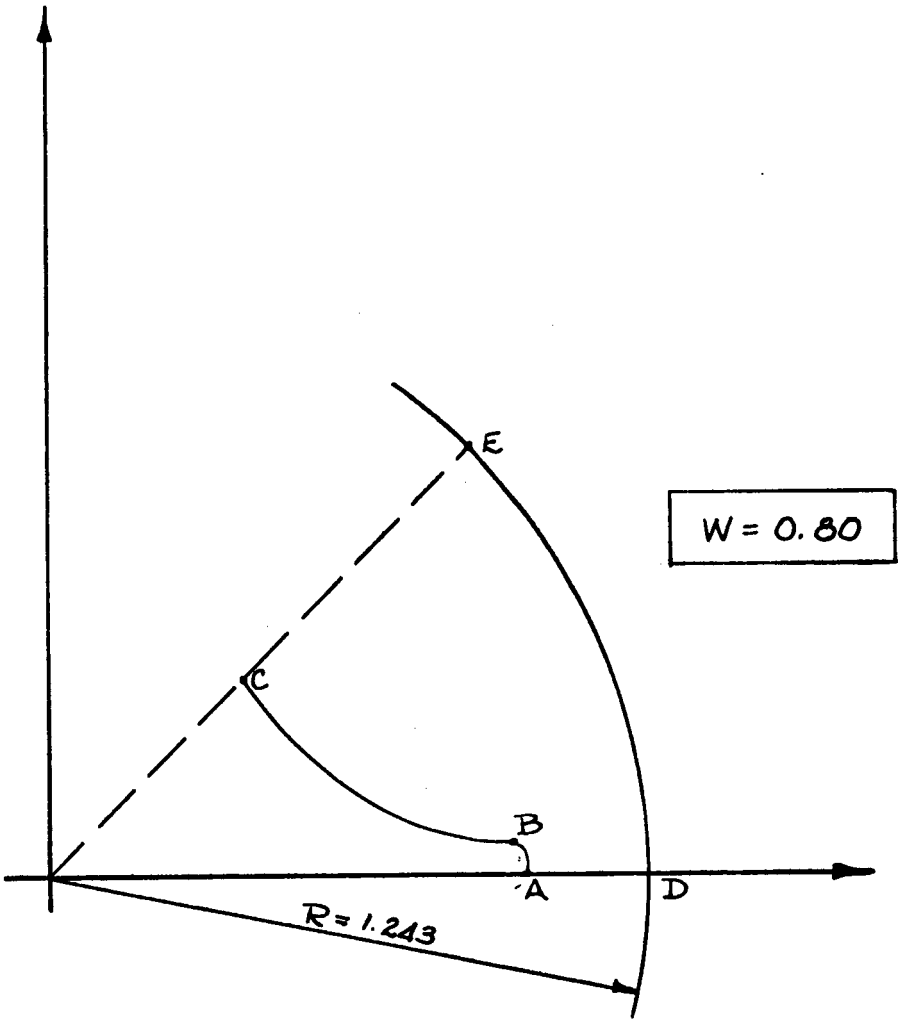

FIGURE 17